AD_____

Award Number: W81XWH-08-2-0157

TITLE: Glyburide-Novel Prophylaxis and Effective Treatment for Traumatic Brain Injury

PRINCIPAL INVESTIGATOR: Dr. J. Marc Simard

CONTRACTING ORGANIZATION: University of Maryland, Baltimore
Baltimore, MD 21201

REPORT DATE: August 2011

TYPE OF REPORT: Annual

PREPARED FOR: U.S. Army Medical Research and Materiel Command
Fort Detrick, Maryland 21702-5012

REPORT DOCUMENTATION PAGE

Form Approved
OMB No. 0704-0188

1. REPORT DATE *(DD-MM-YYYY)*	**2. REPORT TYPE**	**3. DATES COVERED** *(From - To)*
01-08-2011	Annual	7 JUL 2010 - 6 JUL 2011

4. TITLE AND SUBTITLE

Glyburide-Novel Prophylaxis and Effective Treatment for Traumatic Brain Injury

5a. CONTRACT NUMBER

5b. GRANT NUMBER
W81XWH-08-2-0157

5c. PROGRAM ELEMENT NUMBER

6. AUTHOR(S)

Dr. J. Marc Simard

E-Mail: shave001@umaryland.edu

5d. PROJECT NUMBER

5e. TASK NUMBER

5f. WORK UNIT NUMBER

7. PERFORMING ORGANIZATION NAME(S) AND ADDRESS(ES)

University of Maryland, Baltimore
Baltimore, MD 21201

8. PERFORMING ORGANIZATION REPORT NUMBER

9. SPONSORING / MONITORING AGENCY NAME(S) AND ADDRESS(ES)

U.S. Army Medical Research and Materiel Command
Fort Detrick, Maryland 21702-5012

10. SPONSOR/MONITOR'S ACRONYM(S)

11. SPONSOR/MONITOR'S REPORT NUMBER(S)

12. DISTRIBUTION / AVAILABILITY STATEMENT

Approved for Public Release; Distribution Unlimited

13. SUPPLEMENTARY NOTES

14. ABSTRACT

The overall subject of this project is blast-traumatic brain injury (blast-TBI) and the role of the SUR1-regulated NCCa-ATP channel in blast-TBI. The specific objectives of this project include: (1) develop a standardized rat model of blast-TBI to study the direct transcranial effects of blast on the brain, independent of indirect transthoracic effects; (2) determine the role of the SUR1-regulated NCCa-ATP channel in blast-TBI; (3) in normal human volunteers, determine the safety of the SUR1 blocker, glyburide, as it might be used as prophylaxis against blast-TBI. During the third year of this project, we completed a key objective – the evaluation of our cranial-only blast injury apparatus (COBIA) as it relates to the effect of blast exposure on short term vestibulomotor performance and on long term cognitive performance. In addition, we completed experiments looking at the time course for upregulation and downregulation of SUR1 and TRPM4. The most important findings include: (i) SUR1 and TRPM4 begin to appear as early as 2 hours after injury, and are gone by 7 days after injury; (ii) the dose-response curve for blast intensity vs. biological response is very steep, making it difficult to accurately grade sublethal injuries based on peak overpressure alone; (iii) the apneac response immediate following blast is an excellent predictor of short-term vestibulomotor performance and of long term cognitive performance, making it a very useful independent variable for grading sublethal injuries when establishing the dose-response.

15. SUBJECT TERMS

blast-TBI, sulfonylurea receptor

16. SECURITY CLASSIFICATION OF:			**17. LIMITATION OF ABSTRACT**	**18. NUMBER OF PAGES**	**19a. NAME OF RESPONSIBLE PERSON**
a. REPORT	**b. ABSTRACT**	**c. THIS PAGE**			USAMRMC
U	U	U	UU	39	**19b. TELEPHONE NUMBER** *(include area code)*

Table of Contents

Page

INTRODUCTION: Narrative that briefly (one paragraph) describes the subject, purpose and scope of the research.

The overall subject of this research project is blast-traumatic brain injury (blast-TBI) and the role of the SUR1-regulated NCCa-ATP channel in secondary injury following blast-TBI. The specific objectives of this research project may be summarized as follows:

(1) develop a standardized rat model of blast-TBI, to permit study of direct transcranial effects of blast on the brain, independent of indirect transthoracic blast effects;

(2) using this rat model, determine the specific role of the SUR1-regulated NCCa-ATP channel in blast-TBI, including testing whether block of SUR1 using glibenclamide would show a beneficial effect in blast-TBI;

(3) in normal human volunteers, determine the safety of oral glibenclamide as it might be used as prophylaxis against blast-TBI.

BODY: This section of the report shall describe the research accomplishments associated with each task outlined in the approved Statement of Work. Data presentation shall be comprehensive in providing a complete record of the research findings for the period of the report. Provide data explaining the relationship of the most recent findings with that of previously reported findings. Appended publications and/or presentations may be substituted for detailed descriptions of methodology but must be referenced in the body of the report. If applicable, for each task outlined in the Statement of Work, reference appended publications and/or presentations for details of result findings and tables and/or figures. The report shall include negative as well as positive findings. Include problems in accomplishing any of the tasks. Statistical tests of significance shall be applied to all data whenever possible. Figures and graphs referenced in the text may be embedded in the text or appended. Figures and graphs can also be referenced in the text and appended to a publication. Recommended changes or future work to better address the research topic may also be included, although changes to the original Statement of Work must be approved by the Army Contracting Officer Representative. This approval must be obtained prior to initiating any change to the original Statement of Work.

During last year of the project we concentrated our efforts on the following tasks:

1) Evaluation of the best physical and biological parameters of blast-TBI useful for construction of the intensity-response curves.
2) Time course of the upregulation of the SUR1 post blast-TBI to determine optimal glibenclamide treatment regiment.
3) Evaluation of the best short term outcomes to be used to study glibenclamide efficacy in blast-TBI.
4) Evaluation of the best long term outcomes to be used to study glibenclamide efficacy in blast-TBI.
5) Detailed documentation of all blast-TBI procedures to produce Standard Operating Procedures (SOP) for GLP–valid study to determine the effect of glibenclamide treatment on outcome from blast-TBI.
6) GLP training and certification of personnel.

Summary of animal use:
In the time period between 07/02/2010 and 07/01/2011,
total rats used was 127, including 3 naïve, 10 sham, 8 exclusions, and 106 blasted rats

Overall, primary blast deaths 37, (1 overnight death).
From 106 blast TBI's –

81 using the 24.5 cm BDC and charge 4 powerload (28 blast deaths)
4 using the 19.5 cm BDC charge 4 powerload (1 blast death)
2 using the 17 cm BDC charge 4 powerload (1 blast death)
6 using the 23.25 cm BDC charge 4 powerload (3 blast and 1 overnight deaths)
13 using the 27 cm BDC charge 4 powerload (4 blast death)

Objective 1a: establish the usable working range for the "intensity-response" relationship between blast intensity and outcome in our blast-TBI model

A detailed description and validation of the Cranium Only Blast Injury Apparatus (COBIA) to deliver blast overpressures generated by detonating .22 caliber cartridges of smokeless powder was published this year in *J. Neurotrauma* (appended).[1] Our published data demonstrate our central thesis, that exposure of the head alone to severe blast predisposes to significant neurological dysfunction.

Problem encountered

We originally proposed to establish the usable working range for the "intensity-response" relationship between blast intensity and outcome in our blast-TBI model by varying the size of the BDC, which yields peak overpressures that follow the inverse square law (see Fig. 4C of the appended paper). This approach worked well when the outcome measure was death. As seen in Fig. 5A of the appended paper, a nice dose-response relationship was observed.

However, two problems were encountered when we examined sublethal blast. First, the dose-response curve is very steep, making it difficult to accurately grade sublethal injuries. Secondly, the biological response to sublethal blast does not correlate well with peak overpressures. Examination of Fig. 6A of the appended paper shows that we reported what appears to be a "dose-response relationship", but close examination reveals a flaw – the data for apnea are not distributed as one would expect; instead, the data actually fall into two distinct clumps, the first, ~5 sec, was observed with peak overpressures ranging between 425–525 kPa, and the second, ~12 sec, was observed with peak overpressures ranging between 525–650 kPa. This type of clumping is symptomatic of a steep dose-response curve, and precludes the use of peak pressure as a useful independent variable.

This problem is also illustrated by the data shown in Fig. 9A of this report, showing the distribution of apnea duration in 43 rats after blast exposure, all using a 24.5 cm BDC, which generates peak overpressures at the cranium of 544 ± 41.7 kPa (mean±SD). Note the broad distribution of apnea duration (9.5±3.4 sec; mean±SD) despite the uniformity of blast generation parameters, suggesting that individual biological

responses may provide a better measure of blast exposure than the physical parameters of the blast.

Resolution of the problem

We reasoned that a better way to establish a usable working range for the "intensity-response" relationship to blast injury would be to use the immediate biological response of each animal itself – its apneac response – as a measure of the actual blast experience. We reasoned that the duration of apnea reflects the severity of the immediate impact, and thus reflects the "biological intensity" that is sensed. We examined the relationship between apnea and various neurological abnormalities measured at 24 hours and at later times. Indeed, our analysis showed a high degree of correlation between the duration of apnea immediately after blast and short term (24 hours) and long term (21 days) outcomes. (These data are reviewed in detail below; see Objective 1c and 1d).

Proposed implementation in future experiments

As a result, in future experiments we propose to record the apneac response using an apnea monitor, and to use the duration of apnea as the independent measure of blast intensity to be used in constructions our intensity-response relationship.

Objective 1b: determine the time course for SUR1 and TRPM4 upregulation and downregulation post-blast-TBI.

SUR1 and TRPM4 are the regulatory and pore-forming subunits, respectively, of the SUR1-regulated $NC_{Ca\text{-}ATP}$ channel, which is the target of glibenclamide (to be studied in Objective 1c and 1d). This channel and its subunits are not normally expressed but are transcriptionally upregulated post-injury, as we recently reviewed.[2] It is thus important to determine the time course for upregulation of the channel, because this determines the treatment window during which glibenclamide treatment needs to be started. Similarly, it is important to determine the time course of downregulation, because this determines the length of time that treatment must be continued post-injury.

We performed blast-TBI using 24.5 cm^3 BDC and euthanized animals at 5 different times post-injury, to study upregulation (1/2, 1, 2, 4, 8 hr) and at 5 different times post-injury to study downregulation (1, 3, 5, 7, 10 days) of the molecular components of the $NC_{Ca\text{-}ATP}$ channel (SUR1 and TRPM4) . Sagittal sections of the rats that underwent blast were also labeled with cell-specific markers to determine cellular localization of the SUR1 and TRPM4 protein.

SUR1. As early as 2 hours after blast-TBI SUR1 protein was upregulated in microvessels in the brain stem (Fig. 1) and cerebellum (Fig. 2). Levels of SUR1 expression further increased at 8 and 24 hours after the blast-TBI, with predominant localization in capillaries and larger vessels. Vascular localization of newly expressed SUR1 was confirmed by co-localization with laminin, a protein expressed exclusively in the vascular wall (Fig. 3A). In addition, at 8 hours after blast-TBI, upregulation of SUR1 was detected in Purkinje neurons of the cerebellar cortex. The neuronal origin of the

SUR1-labelled cells was confirmed by co-localization of SUR1 with NeuN protein (Fig. 3B), which is specific for neurons. In parallel with the microvasculature, at 2 hours after blast-TBI, upregulation of SUR1 was detected in the ependymal lining of the cerebral ventricles as well as in vessels and epithelial cells of the choroid plexus (Fig.4).

No evidence of upregulation of SUR1 was detected in astrocytes (Fig. 3C). Interestingly, however, study of the astrocyte-specific protein GFAP indicated an apparent downregulation or disruption of this intracellular filament protein as early as 2 hours after blast TBI. This was evident especially in the cerebellum (Fig. 5), where in control animals levels of GFAP are higher compared to the cerebral cortex.

Upregulation of SUR1 in the choroid plexus and ependyma vanished by 24 hours after blast TBI. In contrast, SUR1 in microvessels and in the cerebellar Purkinje neurons peaked at 24 hours and gradually faded away by the 7th day after blast-TBI.

TRPM4. TRPM4 protein expression after blast generally followed that of SUR1. As early as 4 hours after blast-TBI, TRPM4 was upregulated in the ventral regions of the brain stem. Laminin co-localization of TRPM4 indicated that, like SUR1, TRPM4 co-localized strongly to microvascular endothelium (Fig. 6A,B). Similar to SUR1, Purkinje neurons of the cerebellar cortex expressed TRPM4 at 4–8 hours after blast-TBI. Double labeling with antibodies for both proteins showed clear co-localization of TRPM4 and SUR1 in these cells (Fig. 6C). Like SUR1, TRPM4 was appreciable upregulated after blast-TBI in choroid plexus but not ependyma (Fig. 7). Similarly to SUR1, TRPM4 expression after blast-TBI was primarily localized in the caudal parts of the brain with little or no expression in the cerebral cortex, thalamus or hippocampus.

Conclusion. Overall, our data on the time course of upregulation and downregulation of SUR1 and TRPM4 protein suggest that the SUR1-regulated $NC_{Ca\text{-}ATP}$ channel is involved in the pathogenesis of the blast-TBI as early as 2 hours after the blast and continues to be expressed up to 1 week after blast. Thus, these data indicate that newly expressed SUR1 presents itself as a potential therapeutic target for sulfonylurea drugs such as glibenclamide for up to 1 week after blast-TBI.

Objective 1c: determine the effect of glibenclamide treatment on short-term outcome from blast-TBI.

GLP. Prior to beginning the final work on Objective 1c and Objective 1d, numerous SOPs were written (a list of SOP's is appended; details for each are available on request).

All personnel involved in these experiments underwent GLP Training and were certified. Training included Pharmaceutical Training seminars on GLP. GLP training was provided by Jeiven Pharmaceutical Consulting Inc. (Scotch Plains, NJ).

Short-term outcomes. Prior to actually testing the effect of drug treatment, we had to establish which short-term outcome measures could be used to assess the effect of blast exposure, and to establish the "intensity-response" relationship between blast intensity and outcome.

Data were collected from 53 rats, 10 of which were sham-injured and 43 of which were injured using a 24.5 cm BDC, which generates peak overpressures at the cranium of 544 ± 41.7 kPa (mean±SD; n=31). We examined several vestibulomotor function tests, including: beam walk, beam balance, accelerating RotaRod, and spontaneous rearing. Detailed descriptions of these vestibulomotor tests are provided in the SOP's for the GLP study. Outcome measures were assessed at baseline and on days 1, 3, 7 and 14 after blast-TBI.

Conventional Analysis. After blast-TBI, we observed significant deficits in un-coerced (spontaneous Rearing) and in coerced (accelerating RotaRod, beam walk, beam balance) behavioral tasks. Overall, the strongest differences were observed 24 hours after injury. Significant deficits in performance persisted for the 2 weeks of observation for the beam balance and accelerating RotaRod, whereas performance trended toward normalization for rearing and beam walk (Fig. 8).

Dose-response. We used the duration of apnea as the independent variable to examine the "intensity-response" relationship between blast intensity and outcome. Detailed analysis of the outcomes at 24 hours in individual animals showed considerable variability from animal to animal. However, the degree of abnormality in beam walk, beam balance, accelerating RotaRod and spontaneous rearing, measured at 24 hours after blast, was significantly correlated with the duration of apnea recorded immediately after blast (Fig. 9).

Conclusion. This analysis confirmed that immediate post-blast apnea duration is reliable predictor of the short term vestibulomotor outcome, and can be used as the independent variable to establish the "intensity-response" relationship between blast intensity and outcome. Subsequent GLP experiments to be performed during the upcoming year will utilize this approach, with the anticipation that drug treatment with glibenclamide, if successful, will be reflected as a decrease in the slope of the relationship.

Objective 1d: determine the effect of glibenclamide treatment on long-term neurobehavioral outcome from blast-TBI

Long term Outcomes. As with short-term outcomes, prior to actually testing the effect of drug treatment, we had to establish which long-term outcome measures could be used to assess the effect of blast exposure, and to establish the "intensity-response" relationship between blast intensity and outcome.

Tests were performed on the same rats that were used for the short-term outcomes. Outcome measures were assessed beginning on days 14 and continuing through day 21 after blast-TBI.

We examined two cognitive functions, both measured using the Morris water maze: the memory probe following incremental learning, and rapid learning. Detailed descriptions of these cognitive tests are provided in the SOP's for the GLP study.

Conventional Analysis. On days 14–18 after blast-TBI, incremental learning was similar in sham and blast-exposed rats (Fig. 10A). On day 19, the memory probe was significantly worse in blast-exposed rats (Fig. 10B). On day 21 rapid learning was significantly worse in blast-exposed rats (Fig. 10C)

Dose-response. We used the duration of apnea as the independent variable to examine the "intensity-response" relationship between blast intensity and outcome. The degree of abnormality in memory probe and in rapid learning was significantly correlated with the duration of apnea recorded immediately after blast (Fig. 11).

Conclusion. This analysis confirmed that immediate post-blast apnea duration is reliable predictor of the long term cognitive outcome, and can be used as the independent variable to establish the "intensity-response" relationship between blast intensity and outcome. Subsequent GLP experiments to be performed during the upcoming year will utilize this approach, with the anticipation that drug treatment with glibenclamide, if successful, will be reflected as a decrease in the slope of the relationship.

OBJECTIVE 3: in normal human volunteers, determine the safety of oral glibenclamide as it might be used as prophylaxis against blast-TBI.

The SUR1 blocker, glyburide, in normal human volunteers. This activity has been transferred to the University of Washington, St. Louis, due to the fact that the investigator responsible for this experiment has moved there as faculty.

KEY RESEARCH ACCOMPLISHMENTS: Bulleted list of key research accomplishments emanating from this research.

During last year of the project we concentrated our efforts on the following tasks:

1) Evaluation of the best physical and biological parameters of blast-TBI useful for construction of the intensity-response curves.
2) Time course of the upregulation of the SUR1 post blast-TBI to determine optimal glibenclamide treatment regiment.
3) Evaluation of the best short term outcomes to be used to study glibenclamide efficacy in blast-TBI.
4) Evaluation of the best long term outcomes to be used to study glibenclamide efficacy in blast-TBI.
5) Detailed documentation of all blast-TBI procedures to produce Standard Operating Procedures (SOP) for GLP–valid study to determine the effect of glibenclamide treatment on outcome from blast-TBI.
6) GLP training and certification of personnel.

REPORTABLE OUTCOMES: Provide a list of reportable outcomes that have resulted from this research

"Cranium-only Blast Injury Apparatus (COBIA): A Reproducible Model for Sublethal Blast Traumatic Brain Injury with Delayed Cognitive Deficits". Williams, A; Bochicchio, G; Driscoll, I; Keledjian, K; Simard, P; Gerzanich, V; Scalea, T; Simard J.M.
Presented at: American College of Surgeons -Committee on Trauma, Region 3 annual meeting, December, 2010,

First place basic science American College of Surgeons -Committee on Trauma, State of Maryland annual meeting, November, 2010,

Second place basic science Gary P. Wratten Surgical Symposium, May 2011

CONCLUSION: Summarize the results to include the importance and/or implications of the completed research and when necessary, recommend changes on future work to better address the problem. A "so what section" which evaluates the knowledge as a scientific or medical product shall also be included in the conclusion of the report.

Overall, the project has made important strides in demonstrating early vestibulomotor abnormalites and late cognitive abnormalities induced by exposure of the head alone to blast. These are novel, important findings. In addition, we have delineated the time course for upregulation of the pathological target molecule, SUR1. In the upcoming cycle, we will evaluate whether targeting SUR1 with glibenclamide will impact the outcome measures identified here, by changing the slope of the dose-response curve.

REFERENCES: List all references pertinent to the report using a standard journal format (i.e. format used in *Science, Military Medicine*, etc.).

Reference List

(1) Kuehn R, Simard PF, Driscoll I, Keledjian K, Ivanova S, Tosun C, Williams A, Bochicchio G, Gerzanich V, Simard JM. Rodent Model of Direct Cranial Blast Injury. *J Neurotrauma* 2011. PM:21639724

(2) Simard JM, Woo SK, Bhatta S, Gerzanich V. Drugs acting on SUR1 to treat CNS ischemia and trauma. *Curr Opin Pharmacol* 2008; 8(1):42-9. PM:18032110

SUPPORTING DATA: All figures and/or tables shall include legends and be clearly marked with figure/table numbers

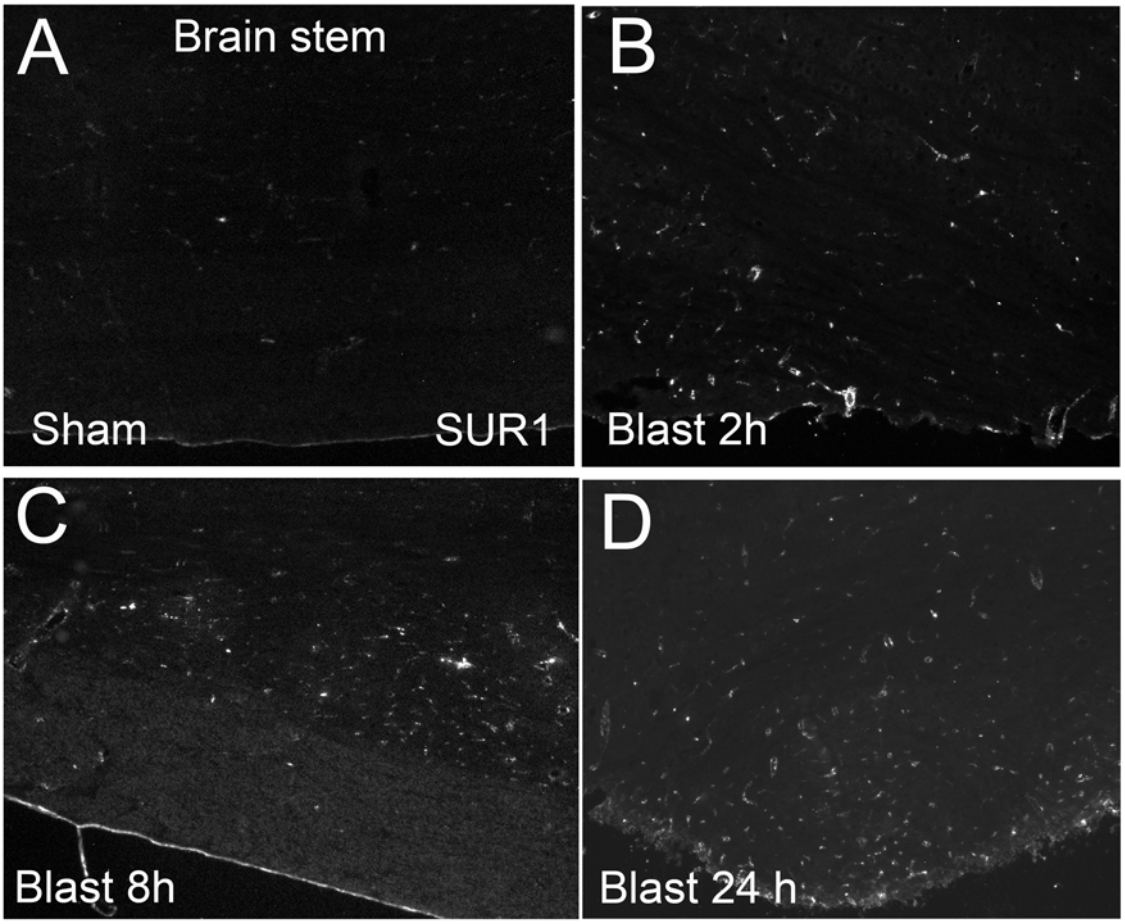

Figure 1. SUR1 is upregulated in brainstem after blast exposure to COBIA. A–D: Low magnification views of sections of the brainstem immunolabeled for SUR1 in sham injured, and blast-injured rats at the times indicated.

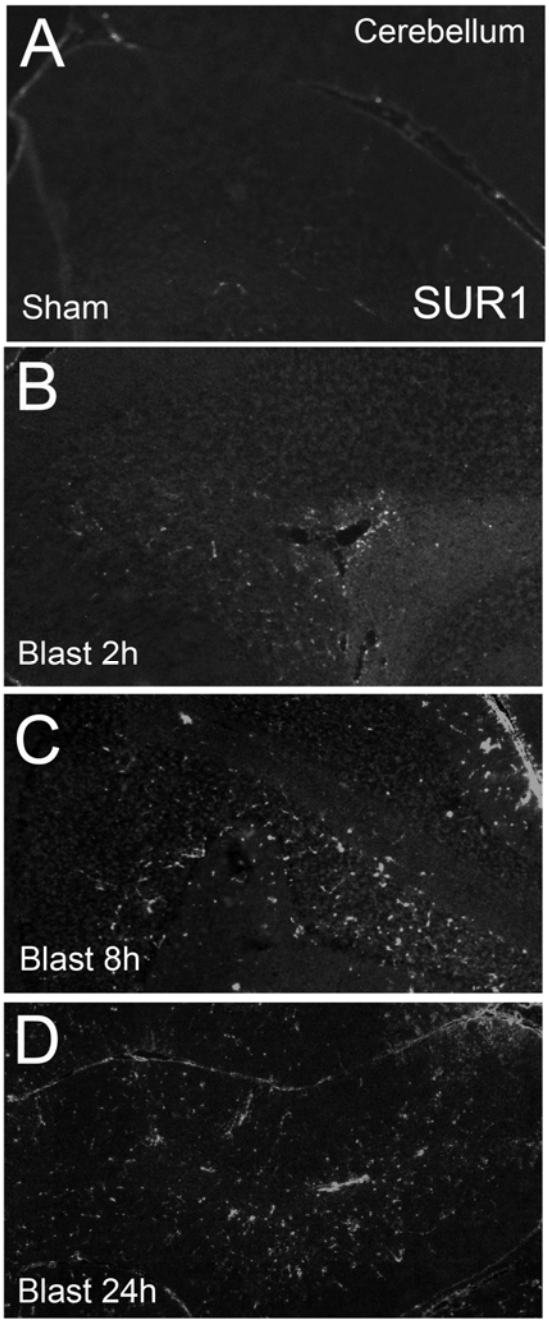

Figure 2. SUR1 is upregulated in cerebellum after blast exposure to COBIA. A–D: Low magnification views of sections of the cerebellum immunolabeled for SUR1 in sham injured, and blast-injured rats at the times indicated.

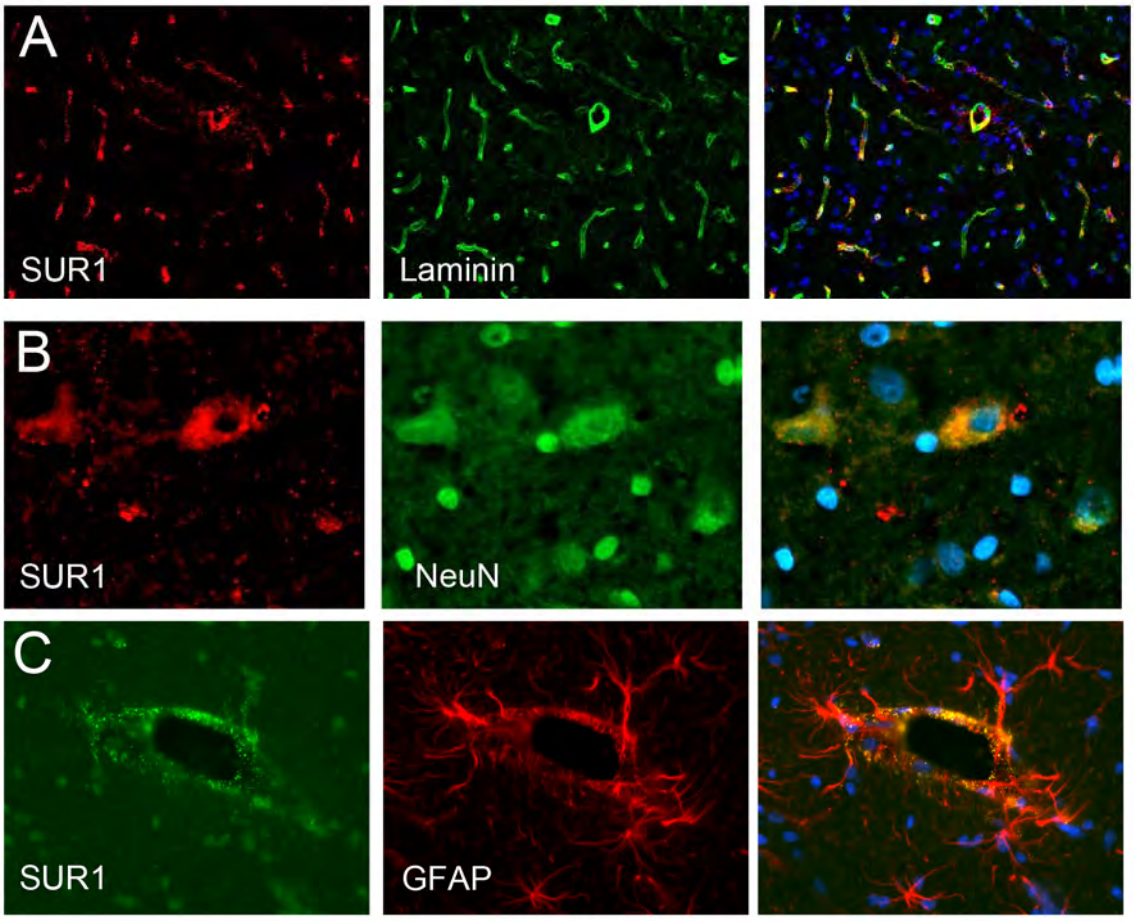

Figure 3. SUR1 is upregulated in microvessels and neurons after blast exposure to COBIA. A–C: High magnification views of sections of the brainstem and cerebellum immunolabeled for SUR1 and co-labeled with laminin to show microvessels (**A**), or Neun to show neurons (**B**), or GFAP to show astrocytes (**C**); note localization of SUR1 in microvessels and neurons, but not astrocytes; panels on the right show the superimposed images from the corresponding images on the left.

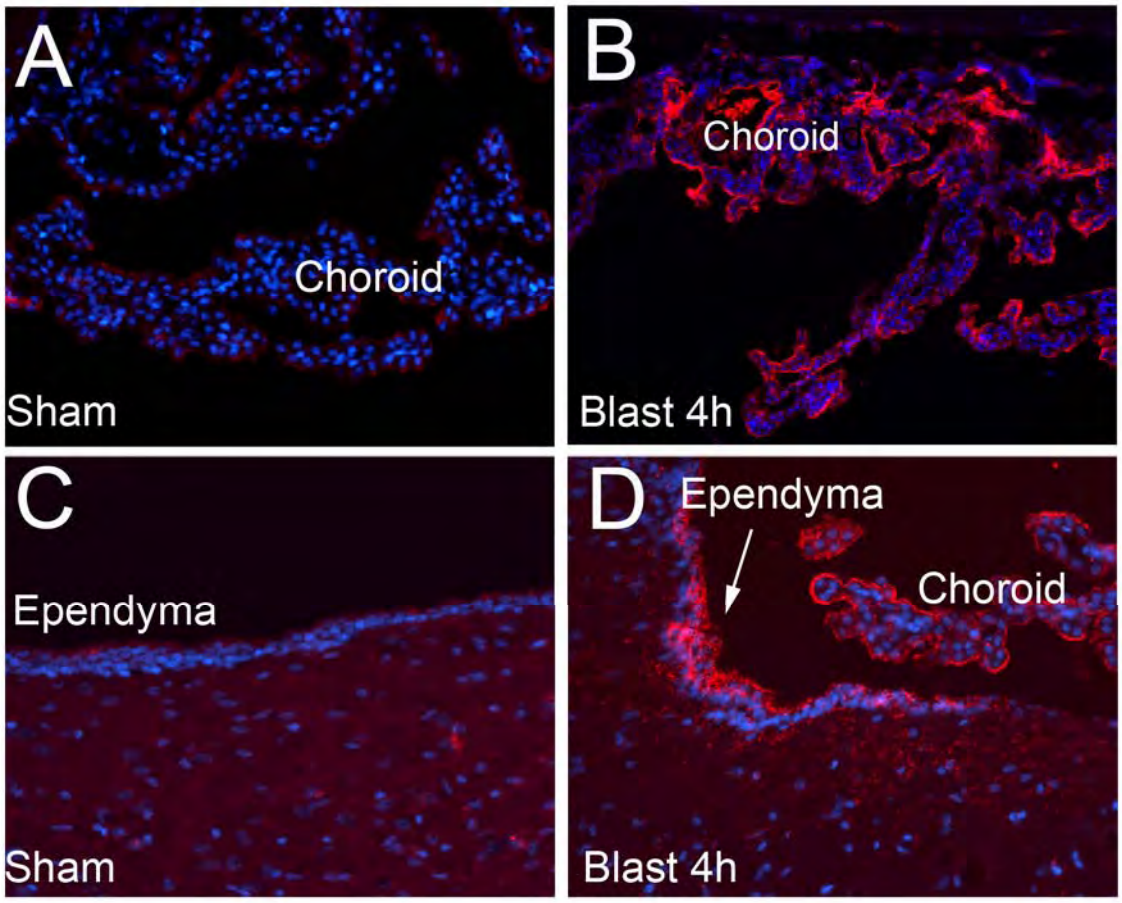

Figure 4. SUR1 is upregulated in choroid plexus and the ependyma after blast exposure to COBIA. A–D: Intermediate magnification views of sections of the ventricles immunolabeled for SUR1 in sham injured (**A,C**), and blast-injured rats (**B,D**); note upregulation of SUR1 in choroid plexus and ependymal lining of the ventricle.

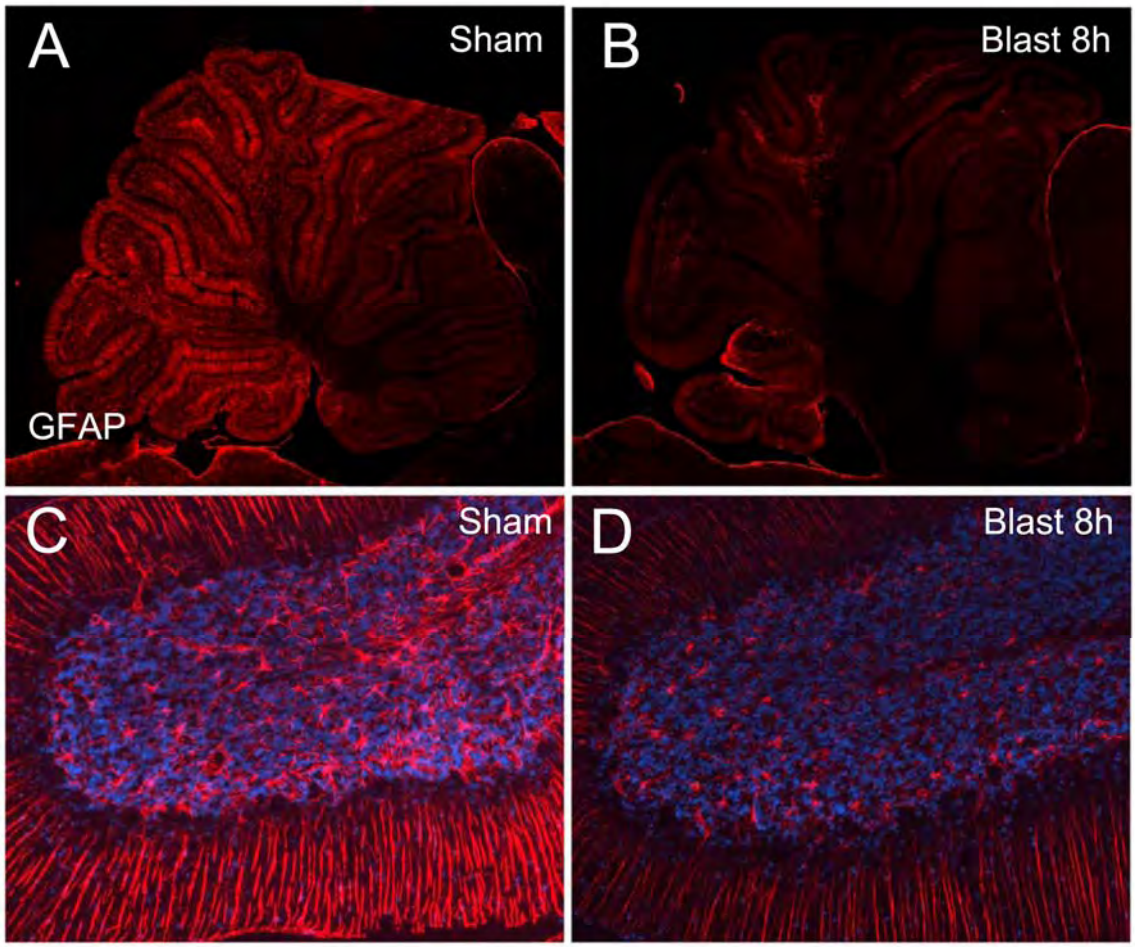

Figure 5. Glial fibrillary acidic protein (GFAP) is downregulated in the cerebellum after blast exposure to COBIA. A–D: Low and high magnification views of sections of the cerebellum immunolabeled for GFAP in sham injured (**A,C**), and blast-injured rats (**B,D**) at the times indicated; note the severe reduction in labeling of astrocyte-specific microfilament protein after blast.

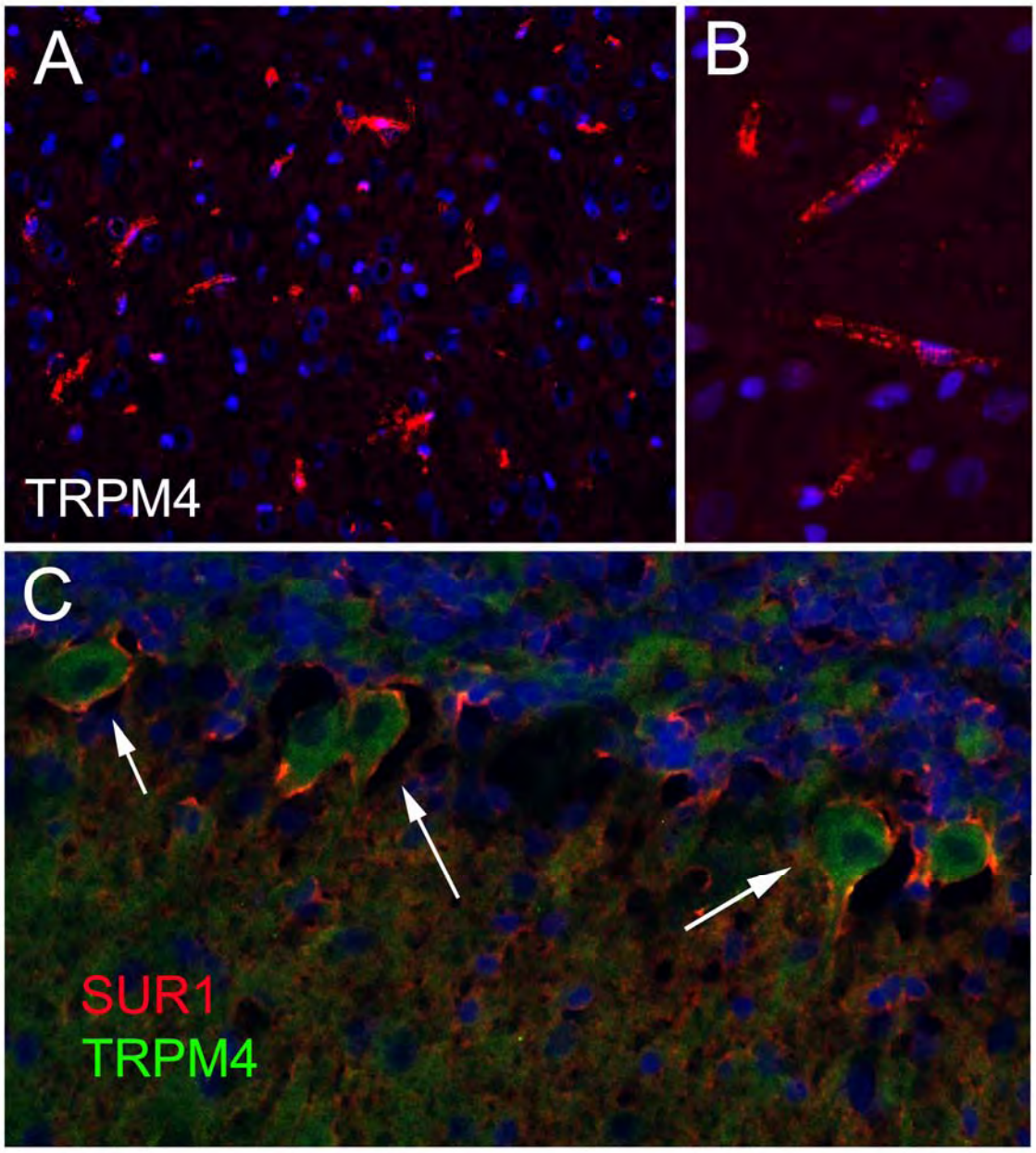

Figure 6. TRPM4 is upregulated in brainstem and cerebellum after blast exposure to COBIA. A,B: Intermediate (**A**) and high (**B**) magnification views of sections of the brainstem immunolabeled for TRPM4 in blast-injured rats, showing labeling in microvessels. **C:** High magnification views of sections of the cerebellum immunolabeled for TRPM4 and SUR1 in blast-injured rats, showing colocalization in Purkinje cells (arrows).

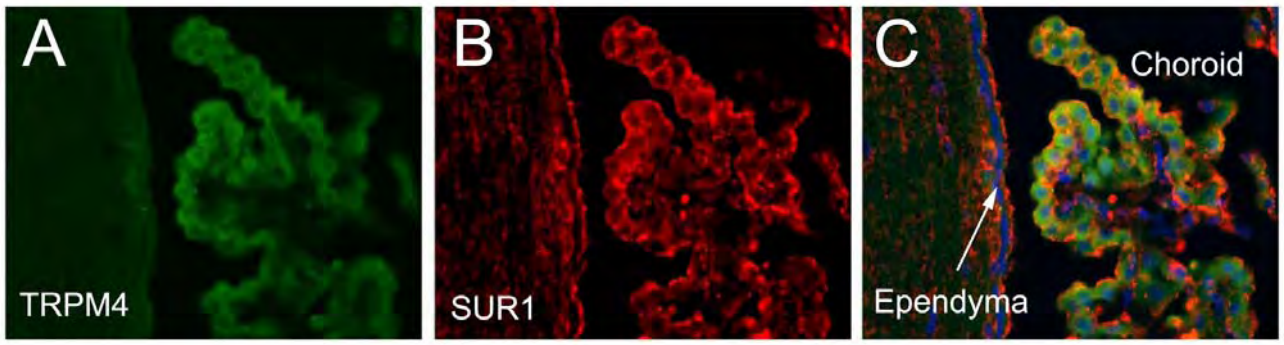

Figure 7. TRPM4 and SUR1 are upregulated in choroid plexus after blast exposure to COBIA. A–C: Intermediate magnification views of sections of the lateral ventricle immunolabeled for TRPM4 (**A**) and SUR1 (**B**) in a blast-injured rat, showing colocalization in the choroid plexus, but not in the ependyma (**C**).

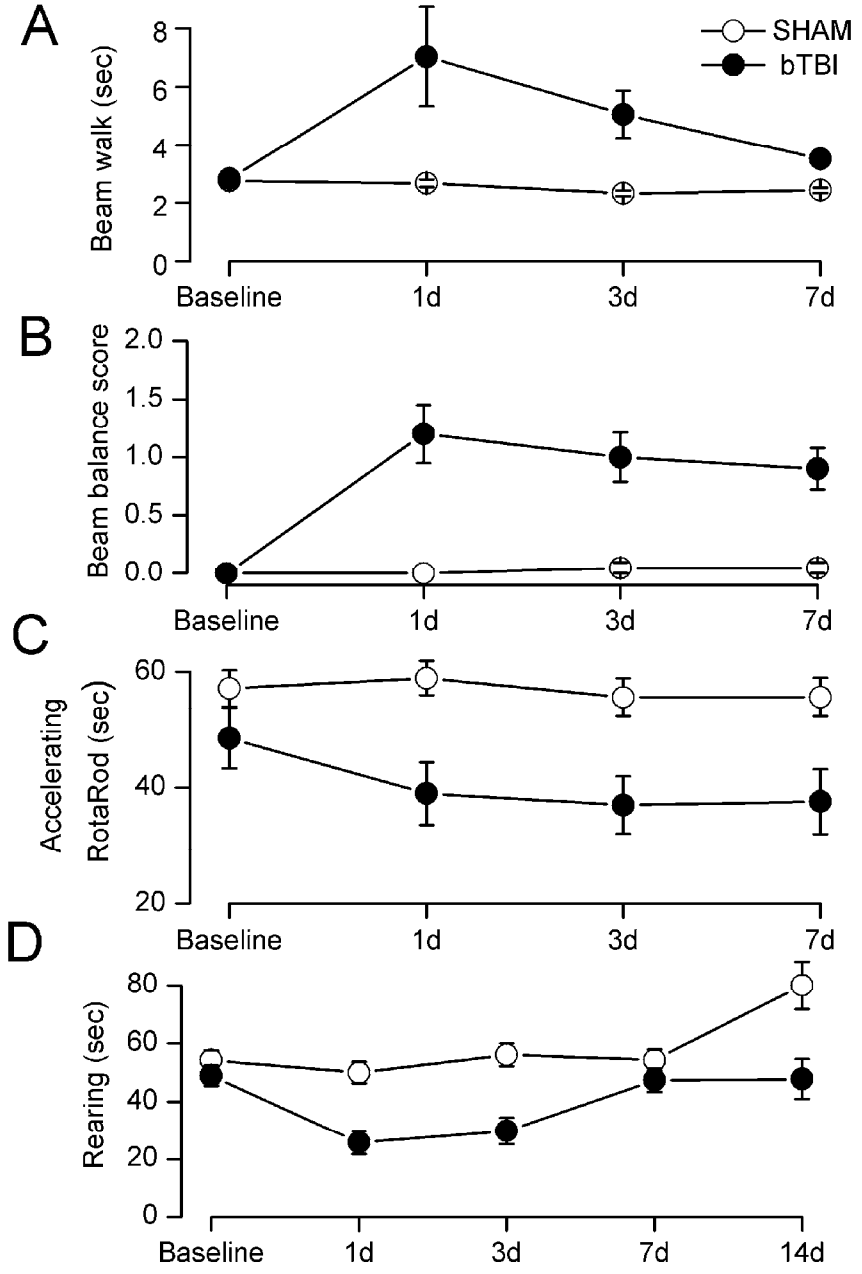

Figure 8. Blast exposure to COBIA causes abnormalities in vestibulomotor performance. A–D: Tests of beam walk (**A**), beam balance (**B**), accelerating RotaRod (**C**) and spontaneous rearing (**D**) over the course of 7–14 days after blast exposure; n=10 sham, 13 blast.

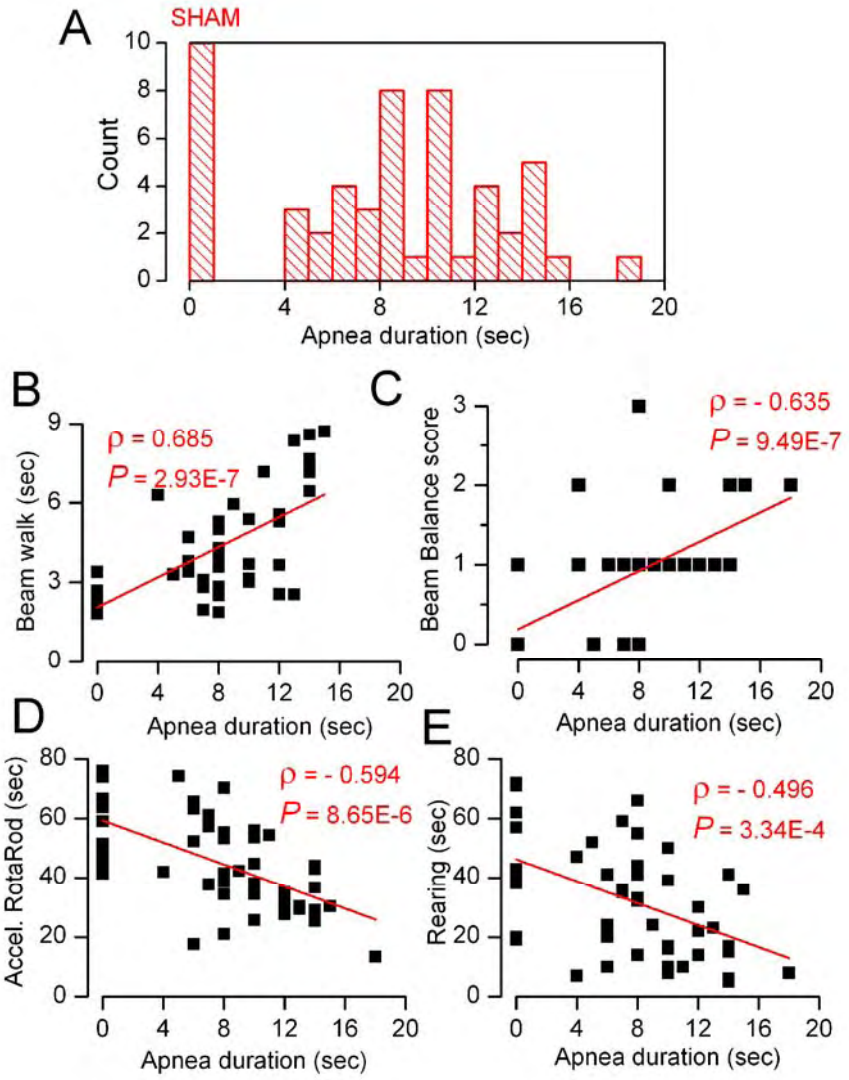

Figure 9. Blast exposure to COBIA causes dose-dependent abnormalities in vestibulomotor performance. A: Histogram of the distribution of apnea duration after blast exposure, all using a 24.5 cm BDC, which generates peak overpressures at the cranium of 544 ± 41.7 kPa; note the broad distribution of apnea duration despite the uniformity of blast generation parameters, suggesting that individual biological responses may provide a better measure of blast exposure than the physical parameters of the blast. **B–E:** Scatter plots of beam walk (**B**), beam balance (**C**), accelerating RotaRod (**D**) and spontaneous rearing (**E**) 24 hours after blast exposure, plotted against duration of apnea; Pearson's correlation coefficient (ρ) and statistical significance (*P*) are also shown; n=53 per test.

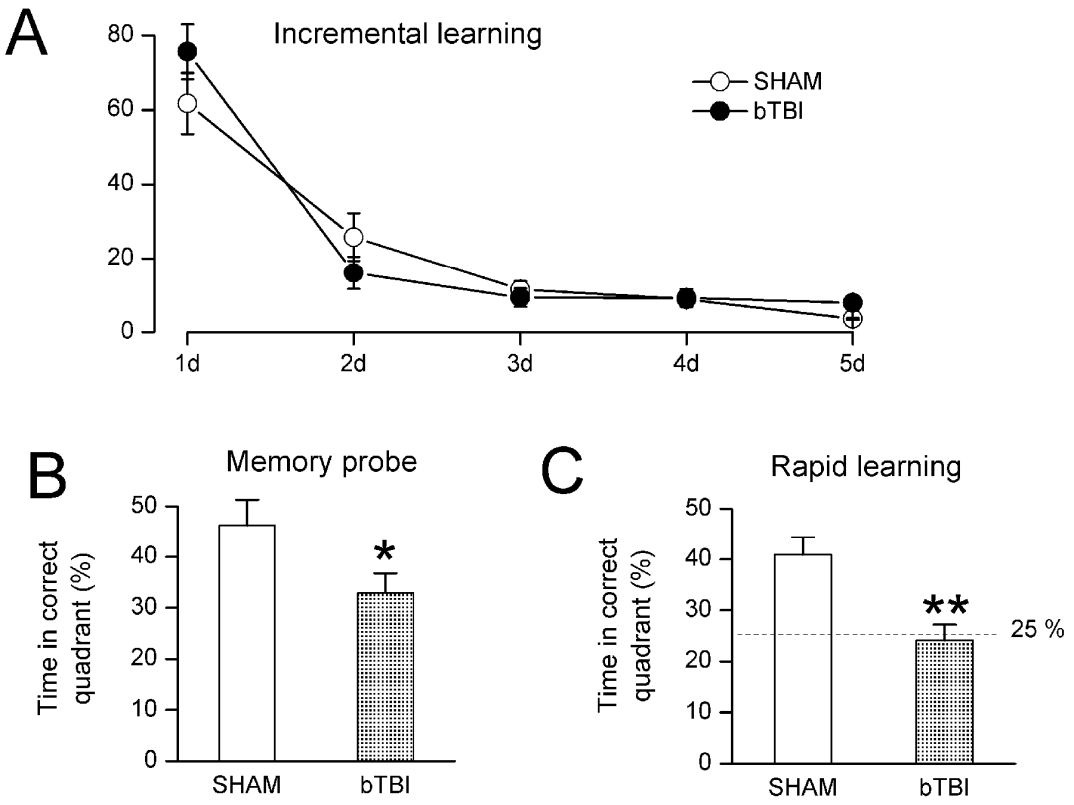

Figure 10. Blast exposure to COBIA causes abnormalities in cognitive performance. A–C: Performance during incremental learning (**A**), at the time of memory probe(**B**), and in rapid learning(**C**) during days 14–21 after blast exposure; n=10 sham, 13 blast.

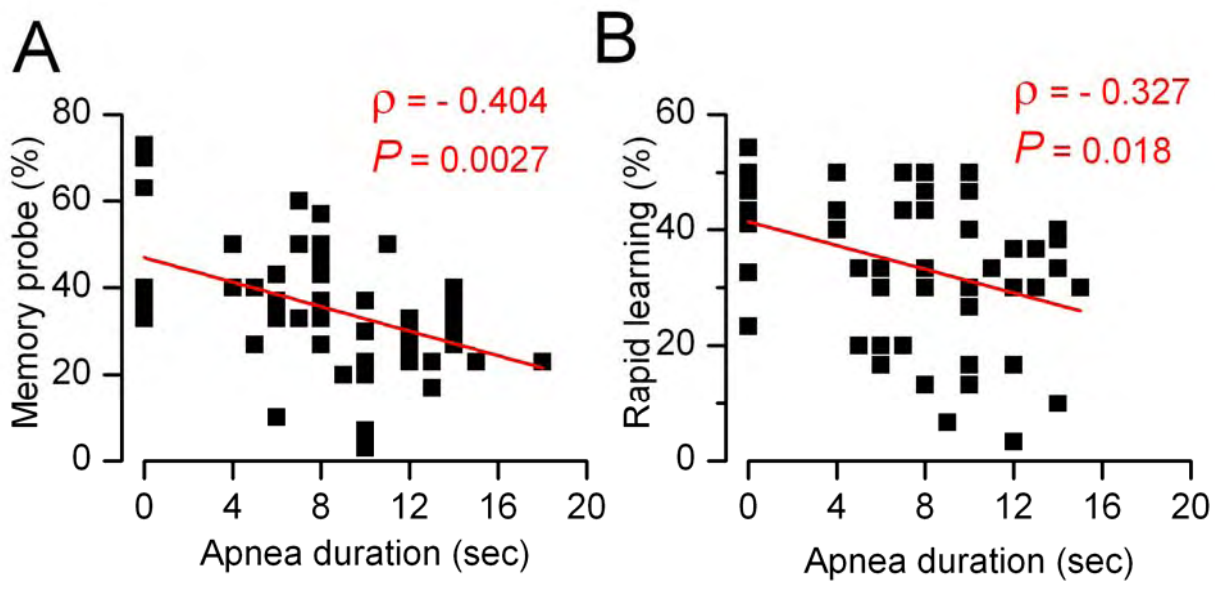

Figure 11. Blast exposure to COBIA causes dose-dependent abnormalities in cognitive performance. A,B: Scatter plots of performance in memory probe (**A**) and in rapid learning (**B**) on days 20 and 21 after blast exposure, plotted against duration of apnea; Pearson's correlation coefficient (ρ) and statistical significance (*P*) are also shown; n=53 per test.

NEU-2010-1532-ver9-Kuehn_1P
Type: Research Article

JOURNAL OF NEUROTRAUMA 28:1–15 (XXXX 2011)

DOI: 10.1089/neu.2010.1532

Original Article

Rodent Model of Direct Cranial Blast Injury

Reed Kuehn,[1] Philippe F. Simard,[2] Ian Driscoll,[1] Kaspar Keledjian,[2] Svetlana Ivanova,[2] Cigdem Tosun,[2] Alicia Williams,[1] Grant Bochicchio,[3,6] Volodymyr Gerzanich,[2] and J. Marc Simard[2,4,5]

Abstract

Traumatic brain injury resulting from an explosive blast is one of the most serious wounds suffered by warfighters, yet the effects of explosive blast overpressure directly impacting the head are poorly understood. We developed a rodent model of direct cranial blast injury (dcBI), in which a blast overpressure could be delivered exclusively to the head, precluding indirect brain injury via thoracic transmission of the blast wave. We constructed and validated a Cranium Only Blast Injury Apparatus (COBIA) to deliver blast overpressures generated by detonating .22 caliber cartridges of smokeless powder. Blast waveforms generated by COBIA replicated those recorded within armored vehicles penetrated by munitions. Lethal dcBI ($LD_{50} \sim 515$ kPa) was associated with: (1) apparent brainstem failure, characterized by immediate opisthotonus and apnea leading to cardiac arrest that could not be overcome by cardiopulmonary resuscitation; (2) widespread subarachnoid hemorrhages without cortical contusions or intracerebral or intraventricular hemorrhages; and (3) no pulmonary abnormalities. Sublethal dcBI was associated with: (1) apnea lasting up to 15 sec, with transient abnormalities in oxygen saturation; (2) very few delayed deaths; (3) subarachnoid hemorrhages, especially in the path of the blast wave; (4) abnormal immunolabeling for IgG, cleaved caspase-3, and β-amyloid precursor protein (β-APP), and staining for Fluoro-Jade C, all in deep brain regions away from the subarachnoid hemorrhages, but in the path of the blast wave; and (5) abnormalities on the accelerating Rotarod that persisted for the 1 week period of observation. We conclude that exposure of the head alone to severe explosive blast predisposes to significant neurological dysfunction.

Key words: β-amyloid precursor protein, caspase-3; primary blast injury; traumatic brain injury

Introduction

Explosive munitions cause more than half of all injuries sustained in military combat, and are responsible for an increasing number of civilian casualties (Aboutanos and Baker, 1997; Belanger et al., 2009; Bochicchio et al., 2008; Coupland and Meddings, 1999; Coupland and Samnegaard, 1999b; Frykberg and Tepas, 1988). Traumatic brain injury due to an explosive blast (blast-TBI or bTBI) is one of the most serious wounds suffered by warfighters in modern conflicts. bTBI can range from overt injuries marked by soft tissue damage to the face and scalp complicated by open brain injury, to more insidious injuries with no external physical damage that manifest as persistent neurocognitive or psychological abnormalities (Belanger et al., 2009; Cernak et al., 1996, 1999a, 1999b; Clemedson, 1956; Denny-Brown, 1945; Elder and Cristian, 2009).

Tremendous progress has been made in understanding the pathophysiology of blast injury (BI) to the brain that is caused by the intense transient overpressure of the blast wave generated by an explosion. Importantly, the so-called "thoracic mechanism" has come to be recognized, whereby the brain is believed to be injured indirectly by a blast wave that impacts the gas-filled thoracic cavity and is transmitted to the brain by way of major blood vessels in the neck (Cernak et al., 1996, 2001; Courtney and Courtney, 2009; Long et al., 2009). Preclinical work has confirmed the importance of protecting against the thoracic mechanism of BI to the brain (Long et al., 2009; Svetlov et al., 2010).

The transmission of a blast wave through the skull to the brain has long been postulated (Clemedson, 1956), but this "direct" mechanism of injury has garnered less attention than the "indirect" thoracic mechanism, owing perhaps to the impression that the brain is protected from direct injury by the relatively rigid skull. However, it has been shown that a blast wave can traverse the cranium of the rat almost unchanged (Chavko et al., 2007). Numerical simulations that take into account the physical properties of the skull and other tissues of

[1]Department of Surgery, Walter Reed Army Medical Center, Washington, D.C.
Departments of [2]Neurosurgery, [3]Surgery, [4]Physiology and [5]Pathology, University of Maryland School of Medicine, Baltimore, Maryland.
[6]R. Adams Cowley Shock Trauma Center, Baltimore, Maryland.

the head exposed to an explosive blast predict that a nonlethal blast can interact with CNS tissues to cause brain injury (Moore et al., 2009; Moss et al., 2009). In principle, a blast wave may induce sufficient flexure of the skull to generate damaging loads within the brain, or it may deposit kinetic energy at boundaries between tissues of different density. Despite such observations and considerations, the effects of an explosive blast overpressure directly impacting the head are poorly understood.

In this study, we sought to investigate the effects of a blast overpressure delivered exclusively to the head, with the aim of determining the effect of direct cranial blast injury (dcBI) uncomplicated by indirect blast injury to the brain mediated by thoracic transmission of the blast wave. We describe and validate a Cranium Only Blast Injury Apparatus (COBIA), which we used to develop a novel rodent model of dcBI in which a blast overpressure is delivered locally to the head, with no exposure of the remainder of the body to the overpressure. In this model, pulmonary injury was absent. Many, but not all, of the neuropathological and neurobehavioral abnormalities reportedly associated with bTBI in humans were observed in this model of dcBI, including prominent subarachnoid hemorrhages, axonal and neuronal injury, and persistent vestibulomotor abnormalities. Notably absent were the brain swelling and delayed death from malignant cerebral edema that have been frequently reported in humans.

Methods

The Cranium Only Blast Injury Apparatus

The COBIA is constructed of several elements (Fig. 1). The central component of the COBIA is a .22 caliber, single-shot, powder-actuated tool (Ramset RS22; ITW Ramset, Glendale Heights, IL). The tool was modified by removing the piston that normally drives the fastener, making the tool function like a firearm and allowing the blast wave to propagate undamped through the barrel. The tool is held vertically using a custom-fabricated stand, which also serves to allow safe use of the tool. The blast is directed downwards into a blast dissipation chamber (BDC), which interfaces snugly with the muzzle of the tool. BDCs of different sizes were used to adjust the magnitude of the blast overpressure that was delivered to the head. The BDCs were fabricated from various lengths of polyvinyl chloride (PVC) pipe (ID 2.05 and 2.54 cm), with the shortest chamber delivering the largest blast overpressure to the head (Table 1). The BDC terminates at the blast dissipation chamber-cranium interface (BDCCI). The BDC-cranium interface is a circular section of PVC pipe (cut from a tee connector; ID 2.54 cm) that holds the rat's head in place. The interface with the scalp is lined with an O-ring made of synthetic foam rubber. The blast wave was generated by firing a .22 caliber crimped brass cartridge (power hammer loads,

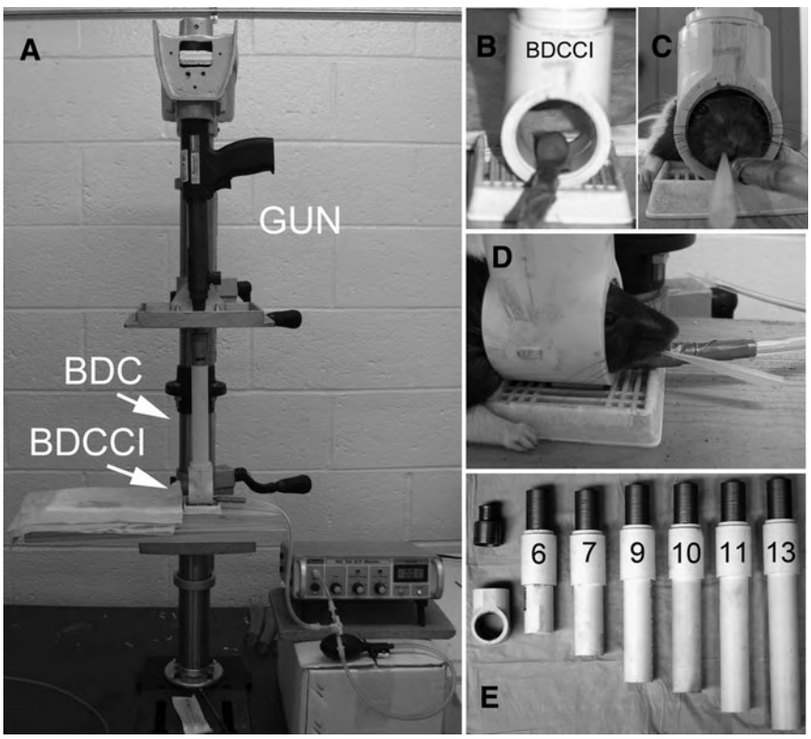

FIG. 1. Cranium Only Blast Injury Apparatus (COBIA). (**A**) Photo of the COBIA showing the vertically-oriented gun interfacing with the blast dissipation chamber (BDC), which connects in turn to the BDC-cranium interface (BDCCI). (**B–D**) Views of the BDCCI before (**B**) and after (**C** and **D**) positioning the intubated, anesthetized rat; note the uninflated balloon in **B,** which when inflated to 10 kPa, promotes contact between the scalp and the O-ring of the BDCCI, resulting in reproducible positioning of the head before injury, and which partially cushions the head during downward acceleration from the blast wind. (**E**) Photo of several of the BDCs used, identified by the numbers referred to in Table 1; to the left is shown the brass coupler that interfaces between the barrel of the gun, the BDC, and the BDCCI.

Table 1. Peak Overpressures with Various Blast Dissipation Chambers (BDCs)

BDC	*Length of BDC (with BDC-cranium interface) (cm)*	*Diameter of BDC (cm)*	*Peak overpressure[1] power level 2 (kPa)*	*Peak overpressure power level 4 (kPa)*
1	9.5	2.05	579	1372
2	10.5	2.05	545	1054
3	14.5	2.05	483	869
4	19	2.05	414	655
5	30	2.05	303	483
6	17	2.54	421	669
7	19.5	2.54	365	655
8	22	2.54	317	545
9	23.25	2.54	303	531
10	24.5	2.54	290	517
11	27	2.54	262	462
12	28.25	2.54	276	448
13	29.5	2.54	269	427

[1]The values shown are the means of 5–10 test firings.

power level 2 or 4, brown and yellow color coding, with 128 ± 4 and 179 ± 5 mg of smokeless powder, respectively).

Measurements of blast waveforms

Pressure measuring system. The overpressures generated by blasts from the COBIA and from the pressure-step generator used for validation (see below) were recorded using a precision dynamic piezoelectric pressure transducer (150 pC/psi; 0.002–12 kHz; Model 100-P; Columbia Research Laboratories, Inc., Woodlyn, PA), and charge amplifier (Model 4601; Columbia Research Laboratories). The transducer was connected to the charge amplifier using a 2-m cable with a 100-pF capacitor in parallel with the input. The output of the charge amplifier was digitized (DigiData 1200, sampling frequency 333 kHz; Axon Instruments, Foster City, CA), and waveforms were stored for offline analysis using pClamp software (version 7; Axon Instruments). The output of the charge amplifier is very sensitive to the setting of the transducer sensitivity control, which adjusts for the total input capacitance, including that for the specific piezoelectric transducer (nominally 150 pF), the input cable (~ 100 pF/m), and the input capacitor (100 pF).

Pressure-step generator. Although the charge amplifier was factory calibrated, we sought to independently verify the calibration for the range of pressures that we would be studying. We constructed a device to generate pressure steps of known magnitude that could be recorded by the pressure measuring system. The pressure-step generator consisted of two chambers, a source chamber and a test chamber, separated by a solenoid-operated valve (#8262G202 120/60, normally closed; Asco, Florham Park, NJ; Fig. 2A). The source chamber (22,712 mL) was pressurized using an air compressor (6 gallon, Model #C2002-WK; Porter-Cable, Jackson, TN), with the exact pressure adjusted to the desired value using a bleed valve, and measured using a factory-calibrated, precision static pressure gauge (4001 heavy duty 4-inch; 0.5% accuracy full scale; Precision Instrument Co., Kennesaw, GA). The test chamber (15 mL) included a valve to allow decompression of the test chamber after each test cycle, and an endcap to interface with the piezoelectric pressure transducer being tested. The apparatus was capable of generating pressure steps from 0 to 600 kPa with a rise time (from 10–90%) of ~ 9 msec. Generating a pressure step did not result in any measureable drop in pressure in the source chamber, due to the large difference in volume between the chambers.

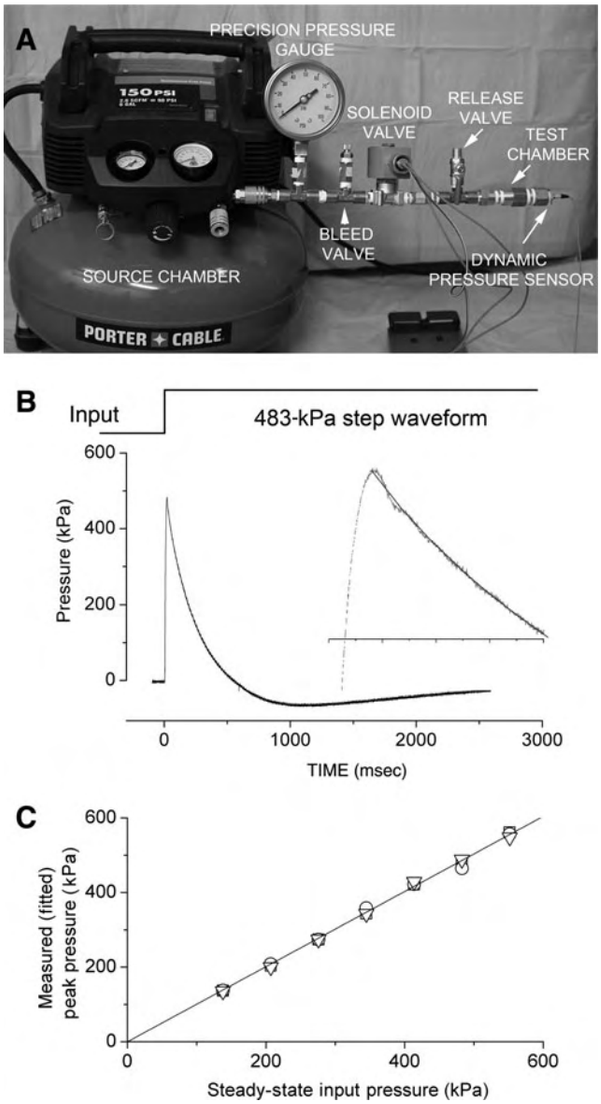

FIG. 2. Validation of the pressure measuring system. (**A**) The pressure step generator used to validate the pressure measuring system (see methods section for description). (**B**) The input pressure step (above) and the output waveform recorded during a validation test run (below); the inset shows the peak of the recorded waveform to illustrate ringing, and the double exponential fit used to estimate the peak value. (**C**) Plot of the steady-state input pressures versus the measured peak pressures estimated from double exponential fits; a least-squares-fit of the data indicated a slope of 1.025 and an intercept of −7.1 kPa, confirming proper calibration of the pressure measuring system.

Validating the pressure measuring system. Pressure steps from 0 to 137.9–551.6 kPa, in increments of 68.9 kPa,

were generated using the pressure-step generator, and were recorded using the pressure measuring system. All measurements were repeated in triplicate. Because the pressure measuring system acts like a second-order bandpass filter, measurements of steady-state pressures were not possible and some ringing of the peak was observed (Fig. 2B). Therefore the decay phases of the recorded waveforms (from the peak out to 1000 msec) were fit with a second-order exponential equation ($\tau 1$, 230–300 msec; $\tau 2$, 50–90 msec) to estimate the peak pressure. Values from the fits were plotted against the steady-state input pressure, showing excellent agreement; a least-squares fit of the data yielded a slope of 1.025 and an intercept of -7.1 kPa (Fig. 2C), confirming proper calibration of the pressure measuring system.

Blast injury procedure

All procedures were approved by the Institutional Animal Care and Use Committee of the University of Maryland School of Medicine. This research was conducted in compliance with the Animal Welfare Act Regulations and other federal statutes relating to animals and experiments involving animals, and adheres to the principles set forth in the Guide for the Care and Use of Laboratory Animals, National Research Council, 1996. Male Long-Evans rats (250–320 g; Harlan, Indianapolis, IN) were anesthetized (60 mg/kg ketamine plus 7.5 mg/kg xylazine, IP), intubated with an endotracheal tube, and were allowed to breathe air spontaneously. Core temperature was maintained at 37°C using an isothermal pad (Deltaphase; Braintree Scientific, Braintree, MA). The hair was clipped from the dorsum of the head.

The rat was positioned prone with the vertex carefully placed against the O-ring of the BDCCI (Fig. 1D). The head was positioned so that when viewed from above, the external occipital crest was $\sim {}^{1}/_{3}$ of the way inside the inner circumference of the BDCCI (Fig. 3A–C). Just prior to detonation, a small balloon under the rat's lower jaw was inflated to 10 kPa to promote contact between the scalp and the O-ring, resulting in reproducible positioning of the head inside the COBIA before the blast. The balloon beneath the jaw also served to cushion (but not prevent) the head from downward acceleration during the blast.

F3 ▶

Positioning the head as described above reduced the exposure to blast of the thin parietal and frontal bones, and of the weakest structures, the sutures between these bones, and allowed the external occipital crest to act as a buttress to prevent inward flexure of the skull during the blast. We assessed for possible inward flexure of the skull, which has been reported in other models (Svetlov et al., 2010), using a thin piece of glass as a strain gauge spanning the sutures exposed to the blast (Fig. 3D). In separate measurements, the glass strain gauge (a cover-slip 0.15 mm thick) was found to fracture by deflecting 0.2 mm midway over a span of 10 mm ($n=6$). After exposing the dorsum of the skull of an anesthetized rat, the glass strain gauge was glued to the skull, centered over lambda, using alpha cyanoacrylate adhesive (Fig. 3D). The scalp incision was sutured and the rat was exposed to a blast overpressure (517 kPa), as detailed above. After the blast, examination of the glass strain gauge revealed no fracture (Fig. 3E), indicating that if inward flexure occurred, it was $<200\ \mu$m at the lambda.

In the usual blast injury procedure, after the blast, the rat was removed from the apparatus and was observed for apnea. If spontaneous respiration did not resume within 10 sec, the endotracheal tube was connected to a ventilator (MicroVent gas, compressed air; Hallowell, Pittsfield, MA), and ventilatory support as well as chest massage were instituted and maintained until either spontaneous cardiopulmonary function resumed or until cardiac arrest was deemed to be irreversible. Survivors were nursed on a heating pad until they recovered spontaneous movements. For sham injury, all of the above was performed except for detonating the cartridge.

Experimental series

Overall we studied 160 rats in two series of experiments: series 1 (79 rats) with BDCs having an internal diameter of 2.05 cm, and series 2 (81 rats) with BDCs having an internal diameter of 2.54 cm. The experiments in series 1 were conducted using BDCs of various lengths and cartridges of power level 2 and 4, and were designed to determine the best combination of BDC size and cartridge power to obtain the desired biological response. Experiments in series 2 were all conducted using cartridges of power level 4, and BDCs of various lengths (all internal diameter 2.54 cm). The 79 rats in series 1 included 62 with dcBI that provided usable data, 4 intended for dcBI that were excluded for various technical reasons (abnormal baseline variables, anesthesia-related death before injury, or improper positioning in the BDCCI), and 13 with sham injuries. Of the 62 with usable dcBI data, 9 died following injury, 11 were euthanized at 24 h, 32 were euthanized at 7 days, and 10 were euthanized at later times. The 81 rats in series 2 included 65 with dcBI that provided usable data, 8 intended for dcBI that were excluded for various technical reasons (as above), and 8 with sham injuries. Of the 65 with usable dcBI data, 25 died following injury, 2 were euthanized at 24 h, and 38 were euthanized at 10 days or beyond.

Physiological measurements

All rats underwent continuous pulse oximetry and heart rate recordings with the sensor placed on the hindlimb (Mouse Ox™; STARR Life Sciences Corp., Oakmont, PA). Readings were taken at baseline, immediately after intubation, and then continuously for 30 min after the injury or sham procedure. A group of 33 rats (7 that died shortly after dcBI, plus 26 rats that survived), underwent cannulation of the tail artery, which was performed after induction of anesthesia and prior to injury; arterial access was used to monitor arterial blood pressure (CyQ; CyberSense Inc., Nicholasville, KY), and in some rats, arterial blood gases (iSTAT; Heska Inc., Loveland, CO).

Neurofunctional testing

The accelerating Rotarod test was used to assess coerced locomotor activity (Hamm, 2001). The rats were placed on the drum of the accelerating Rotarod (starting at 4 rpm, accelerating at a rate of 2 rpm every 5 sec up to a maximum of 45 rpm; IITC, Life Science, Woodland Hills, CA), with 3 trials separated by 20 min administered on each day of testing. We report the average latency to falling off of the drum.

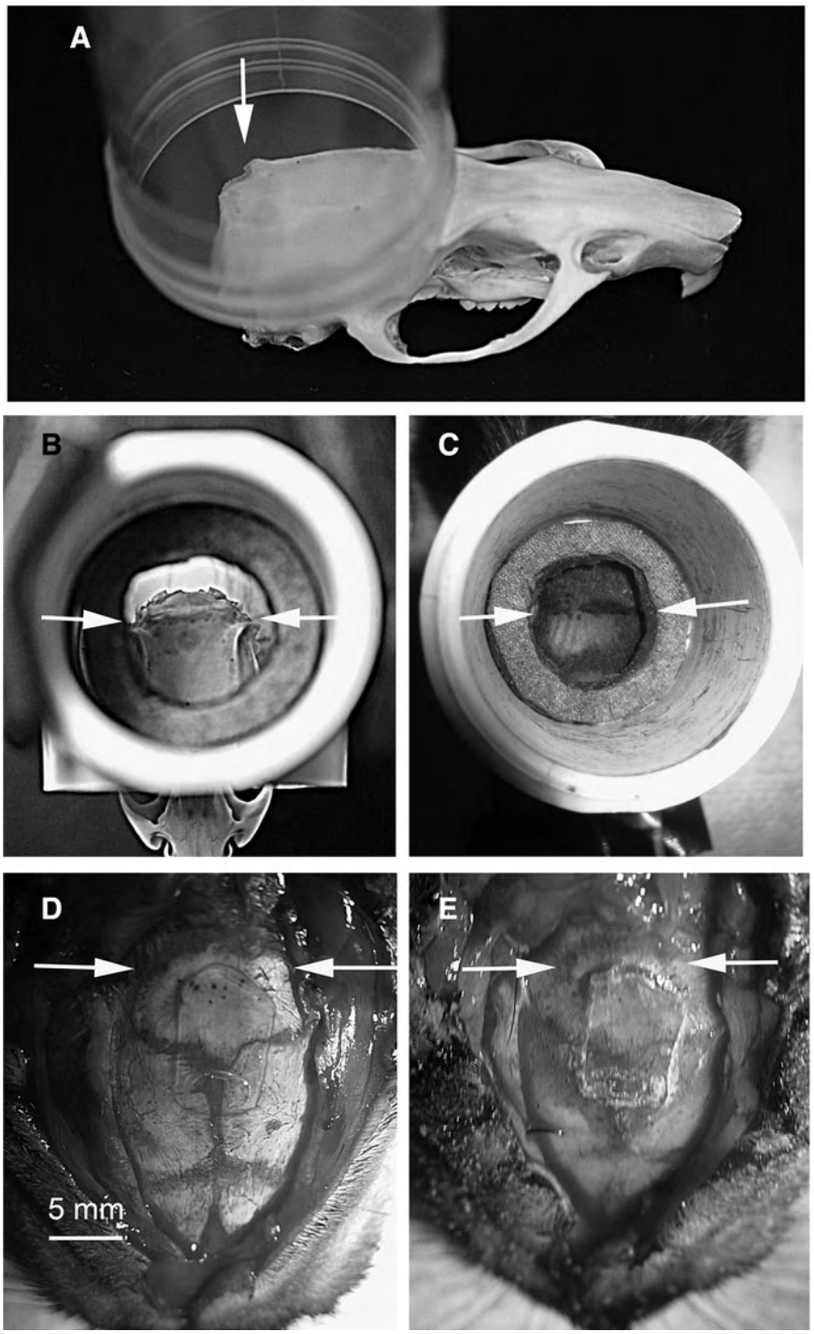

FIG. 3. Positioning of the head inside the Cranium Only Blast Injury Apparatus (COBIA), and absence of significant inward flexure of the skull by the blast. (**A**) Photograph of a rat skull and a clear cylinder (2.54 cm diameter), demonstrating the position of the skull inside the COBIA; note that the external occipital crest (arrow) is situated $\sim {}^{1}/_{3}$ of the way inside the inner circumference of the cylinder, allowing this strong ridge of bone to buttress the skull against inward flexure during the blast. (**B** and **C**) Photographs from above of a rat skull (**B**) and of a live rat head (**C**) positioned inside the blast dissipation chamber-cranium interface (BDCCI) of the COBIA; note the position of the external occipital crest (arrows), which is visually apparent in **B**, and which is marked on the scalp with black ink in (**C**), snout facing downward. (**D** and **E**) Photographs of the thin glass strain gauge glued to the exposed skull over the lambda, before (**D**) and after (**E**) exposure to an explosive blast of 517 kPa; note the absence of fractures in the glass in **E**, indicating that if inward flexure of the skull occurred, it was $<200\,\mu$m at the lambda (see methods section for details), snout facing downward.

Pathology

Necropsies (gross examination of brains and lungs) were performed on all rats that died following dcBI; microscopic examinations (hematoxylin and eosin [H&E] sections) of brains and lungs were performed on 10 rats that died of dcBI, and on 13 rats with sub-lethal dcBI that were euthanized at 24 h. Rats that died shortly after injury were rapidly perfused with saline to remove intravascular contents, and were perfusion-fixed using 4% paraformaldehyde. Rats that survived were euthanized using a lethal dose of pentobarbital IP, after which they were perfused with saline followed by paraformaldehyde fixative, as above. The brains and lungs were harvested and photographed to document subarachnoid hemorrhages and other abnormalities. The fixed brains were cut sagittally and scanned at high resolution to assess for contusions and intraparenchymal or intraventricular hemorrhages. The tissues were then processed for paraffin embedding, sectioned, and stained with H&E for microscopic examination.

Immunohistochemistry

For immunolabeling, perfusion-fixed brains were cryoprotected with 30% sucrose. Cryosections (10 μm) were mounted on slides, blocked in 5% goat serum with 0.2% Triton X-100 in PBS for 1 h, then incubated overnight with primary antibody directed against rat IgG (1:200, catalogue #SC-2011; Santa Cruz Biotechnology, Santa Cruz, CA), β-amyloid precursor protein (β-APP, 1:200, catalogue #51-2700; Invitrogen, Camarillo, CA), or activated (cleaved) caspase-3 (1:200, catalogue #9661; Cell Signaling Technology, Danvers, MA) at 4°C. For fluorescent secondary labeling, the sections were washed three times in phosphate-buffered saline, then incubated in the dark with fluorescent-labeled secondary antibody (1:500, goat anti-rabbit Alexa-Fluor 555; Invitrogen). After 1 h, the slides were washed and cover-slipped with Prolong Antifade reagent with 4,6-diamino-2-phenylindole (DAPI, P36931; Invitrogen). Alternatively, for examining β-APP associated with axonal injury, we used the protocol with diaminobenzidine described previously in this laboratory (Kilbourne et al., 2009). Control experiments included the omission of primary antibody. Low- and high-power photomicrographs were taken using a CoolSNAP camera (Photometrics, Tucson, AZ), and images were adjusted for brightness and contrast using IPLab Software.

Histochemistry

Fluoro-Jade C histo-fluorescence staining was carried out as previously described (Schmued et al., 2005). Briefly, cryosections were first immersed in a solution containing 1% NaOH in 80% EtOH for 5 min. The sections were then rinsed for 2 min each in 70% EtOH and distilled water before being oxidized for 10 min in 0.06% potassium permanganate solution. Following a rinse in distilled water, the sections were stained in 0.0001% Fluoro-Jade C (Chemicon, Temecula, CA), and 0.0001% DAPI (Sigma-Aldrich, St. Louis, MO) solution for 10 min. Finally, the slides were washed 3× with distilled water for 1 min, and dried on a slide warmer at 50°C for 30 min. After clearing in xylene and cover-slipping with nonpolar mounting medium (Cytoseal XYL; Richard-Allan Scientific, Kalamazoo, MI), the sections were examined with an epifluorescence microscope under a fluorescein isothiocyanate (FITC) filter for Fluoro-Jade C signal, with care being taken to limit the time of exposure in order to reduce the likelihood of photobleaching.

Statistical analysis

Unless otherwise noted, values are given as mean ± standard error (SE). Data were analyzed using a repeated-measures one-way analysis of variance (ANOVA) with Bonferroni comparisons. Effects were judged to be statistically significant if $p < 0.05$.

Results

Blast overpressures generated by COBIA

Blast waves generated by the COBIA were measured using a dynamic pressure sensor embedded in a model of the rat head and positioned where the rat's cranium would be in the BDCCI. Recordings of the blast waves showed a large brief transient overpressure, followed by smaller slower transient under- and overpressures that were fully damped within 2 sec (Fig. 4A). At high temporal resolution, the initial overpressure ◀F4 was found to be complex, and included an initial transient lasting 50–100 μsec, followed by a "quasi-static" pressure component. Notably, the initial complex overpressures generated by COBIA resembled published recordings of blast waveforms obtained in an armored vehicle penetrated by a shaped-charge munition (Fig. 4B).

COBIA was designed so that BDCs of different lengths would generate blast overpressures of different magnitude. The average peak overpressures recorded using a variety of BDCs and two different power level cartridges ranged from 250 to >1000 kPa (Table 1). As a first approximation, the magnitudes of the peak overpressures generated using BDCs of different lengths followed the inverse square law (Fig. 4C).

The velocities of the blast waves generated by COBIA were not measured, but could be estimated from fluid dynamic considerations. The relationship between peak overpressure and velocity in air is given by (Harvey et al., 1984; Zel'dovich and Raizer, 1966):

$$P + P_0 = P_0\left[1 + \frac{2\gamma}{(\gamma+1)}\left(\frac{U_s^2}{C^2} - 1\right)\right],$$

where P is the shock overpressure (kPa); P_o is the atmospheric pressure (101.3 kPa); γ is the specific heat ratio (for air, $\gamma = 1.4$); $U^2{}_S$ is the shock velocity (m/sec); and C is the velocity of sound in air (343 m/sec). Thus an overpressure of 500 kPa is estimated to have a supersonic velocity of 784 m/sec.

Lethal blast injury to the cranium

At the time of dcBI, the rats were intubated endotracheally and breathed room air spontaneously. Detonating the cartridge in the COBIA resulted in a blast wind that caused slight downward displacement of the head, which was partially cushioned by the balloon beneath the lower jaw, and a 1–2 cm backward displacement of the head and body. Immediately after lethal dcBI, the rats exhibited opisthotonus (i.e., an extreme, dorsally hyperextended posture of the spine with strong extension of the tail). All rats subjected to dcBI experienced apnea, but with lethal dcBI, apnea was persistent and

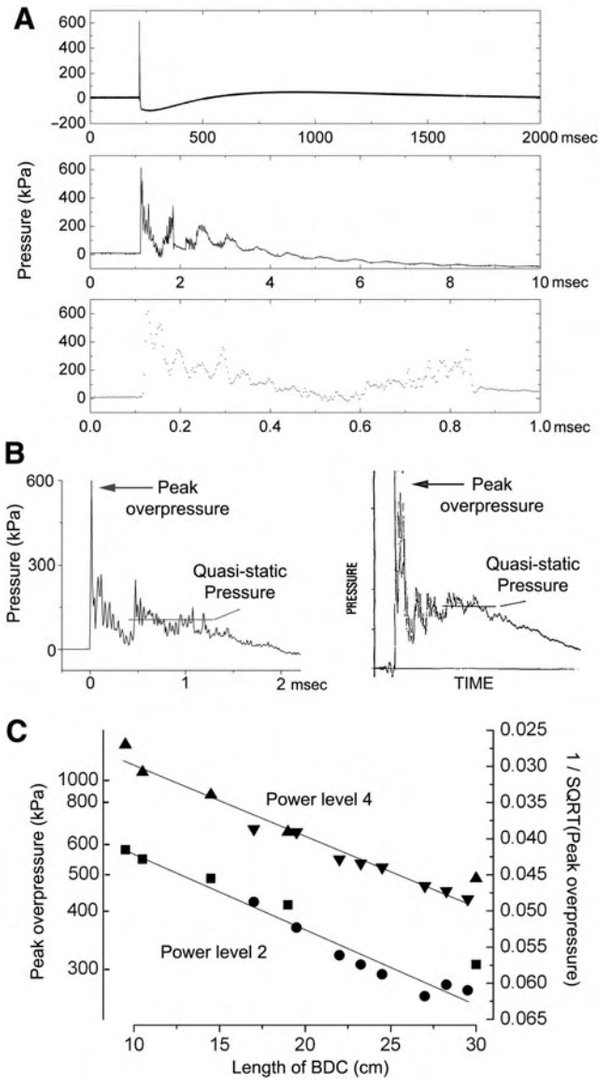

FIG. 4. Pressure waveforms generated by the Cranium Only Blast Injury Apparatus (COBIA). (**A**) Pressure waveforms generated by the COBIA shown at three temporal resolutions, with the lowest resolution showing the typical appearance of a Friedlander wave. (**B**) Comparison of a pressure waveform generated by the COBIA (left), and a published waveform of a blast recorded inside an armored vehicle penetrated by a shaped-charge munition (right; adapted from Stuhmiller et al., 1991). (**C**) Plot of the inverse of the square root (SQRT) of the peak overpressures (right-sided ordinate) generated using blast dissipation chambers (BDCs) of different lengths and cartridges of different power levels, versus the length of the BDC, demonstrating the linear relationship expected for the inverse square law; the values of the peak overpressures are given on the left-sided ordinate (data from Table 1; ■, ▲, BDC internal diameter = 2.05 cm, and ●, ▼, BDC internal diameter = 2.54 cm).

AU3 ▶

was followed within 30–45 sec by cardiac arrest. In 7 rats, continuous monitoring of blood pressure and heart rate using an intra-arterial catheter failed to show any rise in pressure or fall in heart rate during the first 15–30 sec, suggesting the absence of a surge in circulating catecholamines or in vagal tone; systolic blood pressure fell only after cardiac arrest. Mortality was related to the magnitude of the blast overpressure to which the head was exposed. Exposures below 450 kPa were never fatal, whereas exposures to 650 kPa and higher were associated with >85% mortality; the LD_{50} was ~ 515 kPa (Fig. 5A). Fatality was invariably associated with apnea that could not be reversed; mechanical ventilation and cardiac massage never succeeded in resuscitating rats with prolonged apnea (>15 sec). The rapid onset and profound nature of cardiopulmonary arrest following dcBI was consistent with a central mechanism involving the brainstem (i.e., apparent brainstem failure).

◀ F5

Necropsies were performed on all rats with lethal dcBI to further investigate the cause of death. The scalp at the site of maximum blast exposure was always slightly discolored, but showed no evidence of hemorrhage, contusion, or laceration. Subgaleal hemorrhages or contusions of the temporalis muscles were not observed. Examination of the skull, including the coronal, lambdoidal, and sagittal sutures, showed no evidence of injury or weakening of the bones or sutures (Fig. 5B), suggesting the absence of significant inward flexure of the dorsal cranium. All brains excised following lethal dcBI invariably showed extensive subarachnoid hemorrhages, including dorsally over the cerebrum and cerebellum, and ventrally over the entorhinal cortex and brainstem (Fig. 5C). In 10 rats, unprocessed sagittal sections of perfused brains confirmed the presence of subarachnoid hemorrhages, but revealed no apparent cortical contusions or intraparenchymal or intraventricular hemorrhages, and no overt damage to the brainstem (Fig. 5D). Paraffin sections stained with H&E confirmed these findings, including the absence of contusions in the parietal cortex beneath the site of impact of the blast wave and blast wind (Fig. 5E). In five rats, one or two microscopic hemorrhages <200 μm were identified in the brainstem (Fig. 5F). H&E-stained sections of the lungs from 10 rats showed no evidence of overt damage or hemorrhage (Fig. 5G). Thus death was best attributed to brainstem failure due to neural dysfunction in the absence of overt tissue damage.

Notably, rats that survived the initial apneic event almost invariably recovered and survived; delayed deaths were rare. Of the 34 rats that died as a result of dcBI (9 in series 1 and 25 in series 2), all but one in each series died within 1 min of dcBI. The other 2 rats died at ~ 30 min and 12 h, with the specific reason for the delayed death not determined.

Sub-lethal blast injury to the cranium

As noted above, all rats with dcBI became apneic. For survivors, the duration of apnea was generally related to the magnitude of the peak overpressure, and was typically less than 12–15 sec (Fig. 6A).

◀ F6

We monitored standard physiological parameters during the 30 min following sub-lethal blast injury. Sub-lethal dcBI resulted in a significant but brief decline in oxygen saturation attributable to apnea, but no significant changes in blood pressure, heart rate, blood gases, serum electrolytes, or serum glucose (Fig. 6B, C, and D). The absence of any appreciable changes in these variables suggested minimal if any pulmonary effects of the direct cranial blast.

Necropsies were performed at 24 h on 13 rats that survived dcBI (414–655 kPa). Examination of the skull, including the coronal, lambdoidal, and sagittal sutures, showed no

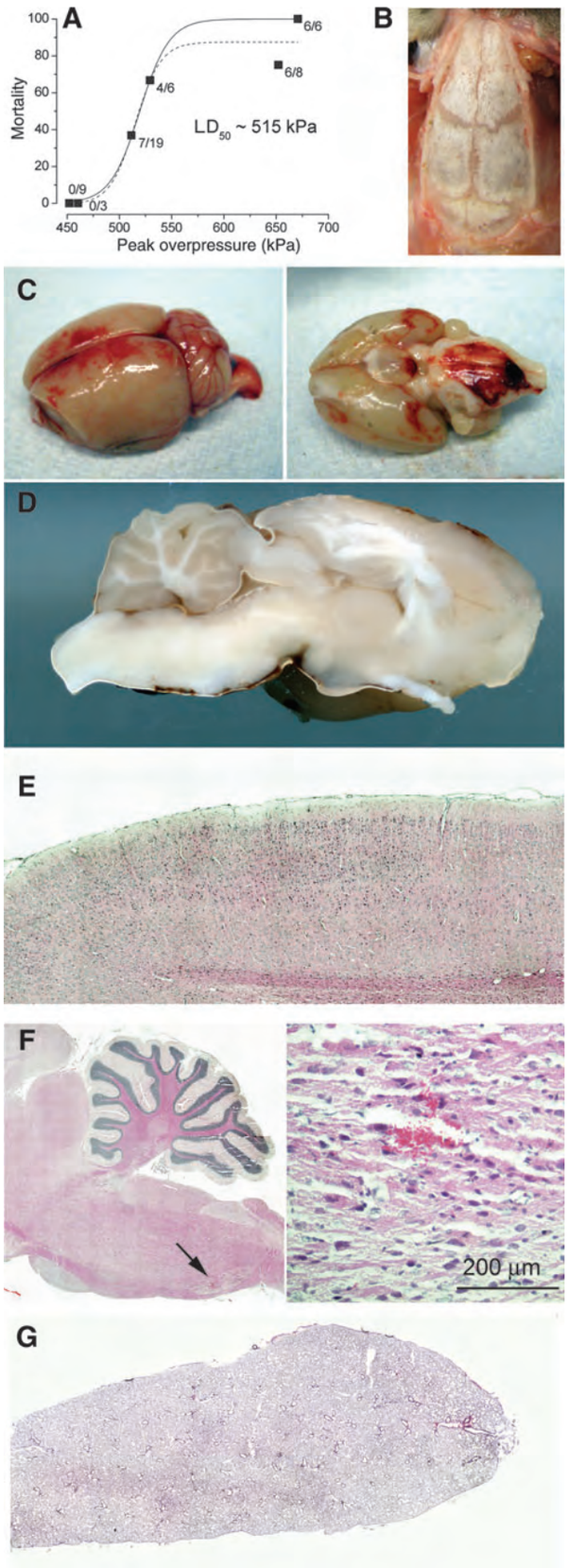

evidence of injury or weakening of the bones or sutures, again suggesting the absence of significant inward flexure of the dorsal cranium. Subarachnoid hemorrhages were an invariant finding, but the amount of blood and the extent of the hemorrhages was less than with lethal dcBI (Fig. 7A). Notably, subarachnoid hemorrhages were evident in the path of the blast wave, including dorsally in mid- and posterior parietal regions of the cerebrum and over the anterior cerebellum, but subarachnoid hemorrhages were not present more rostrally or caudally outside the path of the blast wave (Fig. 7A). As with lethal dcBI, unprocessed sagittal sections revealed no parenchymal hemorrhages, and paraffin sections stained with H&E showed no hemorrhages or contusions of the parietal cortex.

◀ F7

We used IgG immunolabeling as an indicator of microvascular dysfunction. In perfused brains, IgG immunolabeling is normally absent (Fig. 7D). However, IgG immunolabeling may be found under pathological conditions, including: (1) microvascular stasis or thrombosis that prevents intravascular clearance by perfusion; (2) endothelial injury that results in abnormal cellular uptake; and (3) extravasation associated with the formation of vasogenic edema due to breakdown of the blood–brain barrier (Simard et al., 2009a, 2009b). In 8 rats examined at 1–7 days after sub-lethal dcBI (427 and 517 kPa), abnormal IgG immunolabeling was observed in the cerebellum (Fig. 7B and C), and in the thalamus (Fig. 7E and F). In some areas, diffuse labeling was consistent with small regions of vasogenic edema (Fig. 7C and E). Most striking, however, was the unexpected paucity of evidence of vasogenic edema in these brains. In most instances, distinct microvascular labeling without extravasation appeared to be attributable to microvascular stasis or thrombosis, or possibly abnormal endothelial uptake, although post-mortem perfusion artifact could not be completely discounted (Fig. 7B and F).

4C ▶

Immunolabeling for IgG showed a consistent abnormality in the entorhinal cortex. Typically, the ventral-most tip of both temporal lobes exhibited a distinct region of abnormal IgG

FIG. 5. Lethal direct cranial blast injury (dcBI). (**A**) Plot of the percent mortality versus peak overpressure, showing a 50% lethal dose (LD_{50}) of ~ 515 kPa; data from 51 rats, all obtained with blast dissipation chambers (BDCs) of 2.54 cm internal diameter (series 2). (**B**) Image of the exposed skull at the site of maximum blast exposure immediately following lethal dcBI, showing no signs of inward flexure or of other injury to the bones or sutures. (**C**) Images of dorsal and ventral brain surfaces showing extensive subarachnoid hemorrhages following lethal dcBI. (**D**) Images of unprocessed parasagittal sections of the brain, showing the absence of cortical contusions and of other internal hemorrhages following lethal dcBI. (**E**) Hematoxylin and eosin (H&E)-stained sections of the parietal cortex in the path of the blast wave, showing an absence of cortical contusions. (**F**) H&E-stained sections of the cerebellum and brainstem following lethal dcBI, mostly confirming the absence of internal brain hemorrhages (left), but occasionally showing one or two microhemorrhages $<200\,\mu$m (arrow on the left image, and magnified view on the right). (**G**) H&E-stained sections of the lungs following lethal dcBI, showing normal-appearing parenchyma. In all cases, the brains and lungs were harvested and imaged shortly after death, which occurred within 2 min of the blast injury.

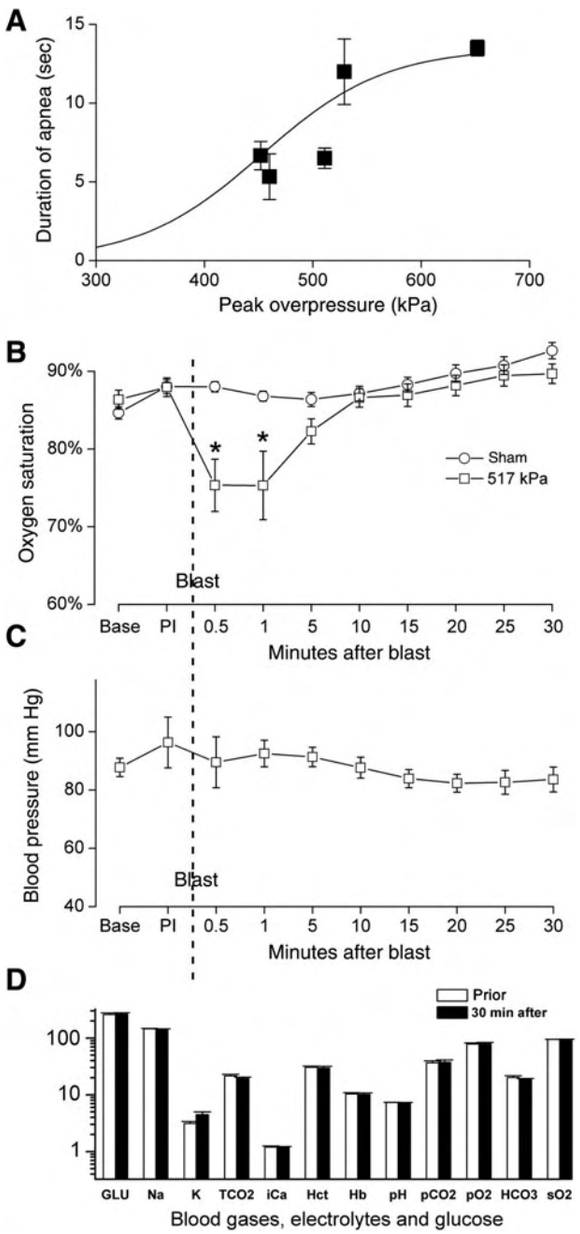

FIG. 6. Sub-lethal direct cranial blast injury (dcBI). (**A**) Plot of the duration (mean ± standard error) of apnea versus peak overpressure; data are from 3–12 rats at each point; 30 rats total. (**B**) Plot of the oxygen saturation during the initial 30 min following sub-lethal dcBI (517 kPa) in 13 sham and 17 injured rats (*$p < 0.05$). (**C**) Plot of systolic blood pressure during the initial 30 min following sub-lethal dcBI (427–517 kPa; 26 rats). (**D**) Bar graphs comparing blood gases, serum electrolytes, and serum glucose before and 30 min after dcBI (427–517 kPa; 17 rats); all values were normal before injury, and except for potassium, were not significantly affected by injury; the slight elevation in potassium was attributed to hemolysis due to clotting in the indwelling catheter (GLU, glucose; Na, sodium; K, potassium; TCO2, total carbon dioxide; iCa, ionized calcium; Hct, hematocrit; Hb, hemoglobin; pCO2, partial carbon dioxide pressure; pO2, partial oxygen pressure; HCO3, bicarbonate; sO2, oxygen saturation).

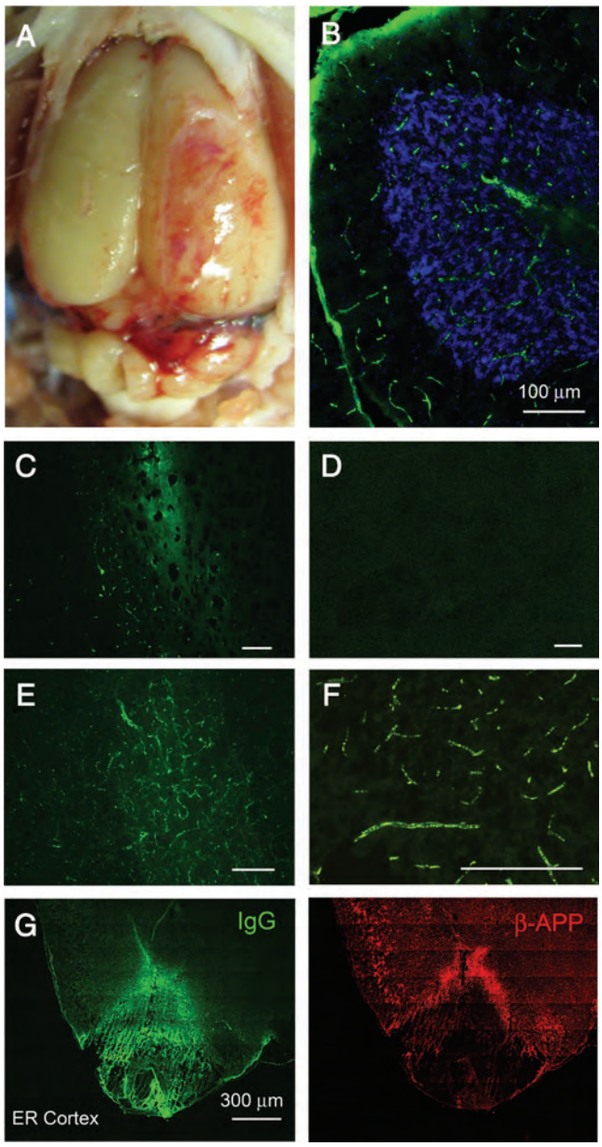

FIG. 7. Sub-lethal direct cranial blast injury (dcBI): microvascular abnormalities and contrecoup injury. (**A**) Image of the dorsal surface of the brain 24 h after sublethal dcTBI (427 kPa), showing the presence of subarachnoid hemorrhage involving the cerebellum and parietal lobe in the path of the blast wave, but sparing the rostral cortex outside of the path. (**B**–**F**) Cryosections of cerebellum (**B**–**D**) and thalamus (**E** and **F**) immunolabeled for rat IgG 24 h after sub-lethal dcBI (517 kPa in **B**, **C**, **E**, and **F**), or following sham injury (**D**), showing no labeling in uninjured controls (**D**), a diffuse pattern of labeling suggestive of vasogenic edema (**C** and **E**), or distinct microvascular labeling consistent with stasis or thrombosis (**B** and **F**). (**G**) Cryosection of entorhinal cortex (ER Cortex) immunolabeled for rat IgG and co-labeled for β-amyloid precursor protein (β-APP), showing contrecoup injury at the ventral tip with surrounding penumbral vasogenic edema and β-APP upregulation 24 h after sub-lethal dcBI (517 kPa).

◀4C

extravasation, with the superior aspect of this region marked by a zone of excess labeling for β-APP (Fig. 7G). These findings correlated with the gross examination of these brains, which consistently showed a ring-like pattern of subarachnoid hemorrhage surrounding the ventral tip of the temporal lobes (see Fig. 5C, right panel). This pattern of injury was suggestive of a contrecoup injury, which could have resulted from downward acceleration of the head by the blast wind impacting the dorsal cranium, but a direct effect of the blast wave itself could not be excluded.

Several deep brain regions that were distant from the subarachnoid hemorrhages showed consistent elevations in nuclear cleaved caspase-3, including cerebellum, hippocampus, brainstem, and corpus callosum (Fig. 8A–D). Quantification of the number of nuclei with cleaved caspase-3 in these regions showed significant elevations compared to uninjured controls (Fig. 8E).

After axonal injury, persistent axonal transport upstream of the injury leads to bulbous accumulations of β-APP in damaged axons (Blumbergs et al., 1995; Bramlett et al., 1997; Pierce et al., 1996; Stone et al., 2000). In addition, injured neurons may exhibit an increase in cytoplasmic β-APP in their perikarya (Itoh et al., 2009; Kilbourne et al., 2009). We examined β-APP immunolabeling in 8 rats 7 days after sub-lethal dcBI (517 kPa). In only 2/8 rats examined we found abnormal beaded accumulations of β-APP consistent with axonal damage in deep white matter in the path of the blast wave (Fig. 9A), suggesting that axonal injury is not a prominent feature in this model. In all rats, upregulation of β-APP was evident in cells deep to the surface, away from subarachnoid hemorrhages, including cerebellar Purkinje cells and hippocampal neurons (Fig. 9B). Notably, regions with cellular upregulation of β-APP coincided with regions that stained for Fluoro-Jade C (Fig. 9C and D), a marker of cell degeneration. These findings also correlated with regions that labeled strongly for nuclear cleaved caspase-3 (Fig. 8A and B).

We used the accelerating Rotarod task to gauge neurological function. Following sub-lethal dcBI (427 and 517 kPa), performance was significantly degraded compared to controls, with the abnormality persisting for the entire week of observation (Fig. 9E).

Discussion

Blast injury is classified into four phases, each of which can result in brain injury (http://www.bt.cdc.gov/masscasualties/explosions.asp). Primary blast injury (PBI) is caused by the blast wave itself. Secondary blast injury results from ballistic fragments penetrating into the head or body. Tertiary blast injury is caused by the "blast wind," a forceful air flow that accelerates the head and body and can cause impact/acceleration injuries. Quaternary blast injury incorporates other mechanisms including hemorrhagic shock and chemical or thermal injuries (Chen et al., 2009). Of the four mechanisms, only the first, PBI, is unique to an explosive blast; the last three cause TBI and other bodily injuries that are indistinguishable from those encountered in settings unrelated to blast. Within this complex compilation of mechanisms of bTBI, the least well understood is PBI. Emerging research suggests that PBI involving the brain may be divisible based on two distinguishable mechanisms: direct PBI due to the blast wave striking the cranium proper, and indirect PBI due to the thoracic mechanism.

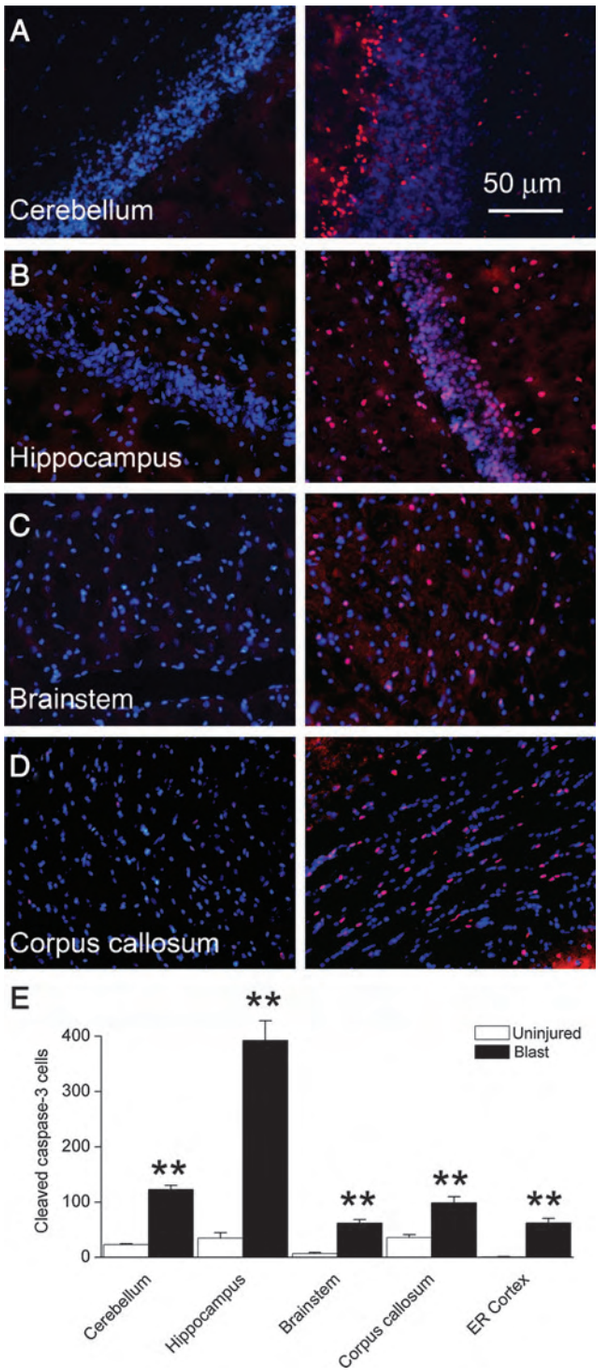

FIG. 8. Sub-lethal direct cranial blast injury (dcBI): cleaved caspase-3. (**A–D**) Cryosections of cerebellum, hippocampus, brainstem, and corpus callosum from uninjured rats (left column) and from rats 24 h after sub-lethal dcBI (517 kPa), immunolabeled for cleaved caspase-3 (red), and stained with 4,6-diamino-2-phenylindole (DAPI, blue) to show nuclear localization of cleaved caspase-3. (**E**) Counts of nuclei with cleaved caspase-3 in various brain regions including the entorhinal cortex (ER Cortex), from uninjured rats (open bars), and from rats 24 h after sub-lethal dcBI (517 kPa; solid bars); counts were obtained in regions of interest 400 × 400 μm for each area for each of 5 rats (**$p < 0.01$).

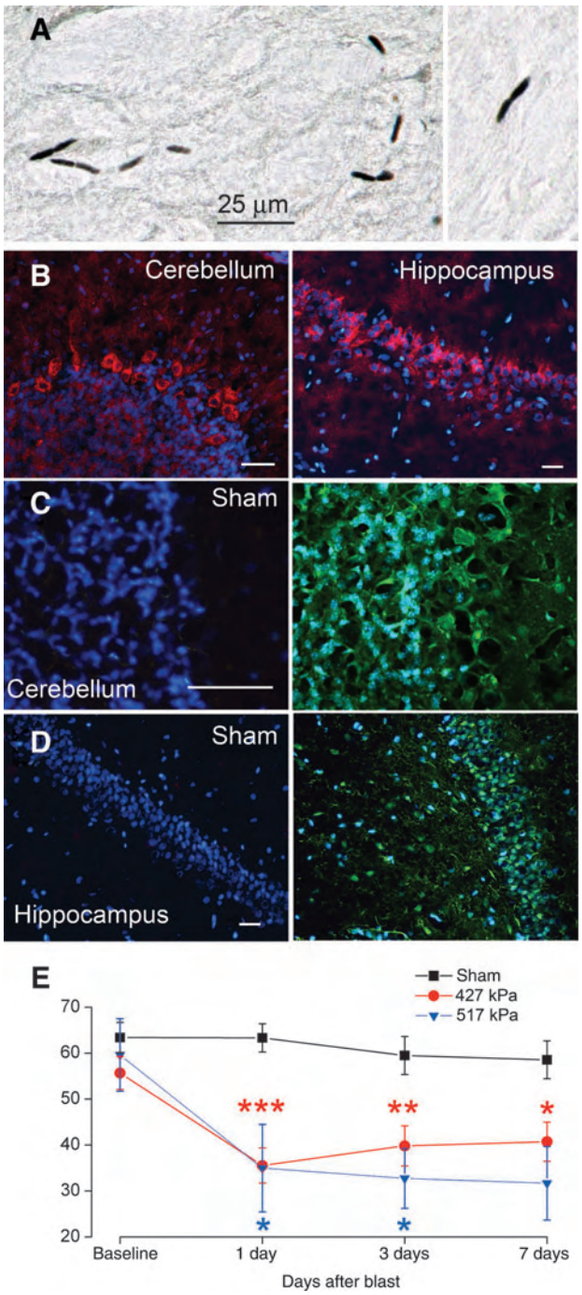

4C ▶

FIG. 9. Sub-lethal direct cranial blast injury (dcBI): axonal and neuronal abnormalities and neurological dysfunction. (**A**) Cryosections immunolabeled for β-amyloid precursor protein (β-APP) (visualized with diaminobenzidine), showing axonal disruption in deep white matter. (**B**) Cryosections immunolabeled for β-APP (visualized with fluorescent secondary antibody), showing upregulation in cerebellar Purkinje cells and hippocampal neurons. (**C** and **D**) Cryosections stained with Fluoro-Jade C, showing positive labeling in cerebellar Purkinje cells and hippocampal neurons from injured rats (right) but not in uninjured rats (left); all scale bars = 25 μm. (**E**) Performance on the accelerating Rotarod in sham-injured rats ($n = 16$), and in rats with sub-lethal dcBI (427 kPa, $n = 14$; 517 kPa, $n = 5$), showing significant abnormalities that persisted for the entire week of testing (*$p < 0.05$; **$p < 0.01$; ***p ????).

AU4 ▶

In general, it is likely that most models of bTBI that utilize shock tubes or open field exposures to explosive blasts (Long et al., 2009; Svetlov et al., 2010) result in combinations of direct PBI, indirect PBI, and tertiary blast injury to the brain, the latter due to acceleration of the head by the blast wind. The model that we developed and validated here using the COBIA was designed specifically to eliminate indirect PBI to the brain mediated by thoracic transmission of the blast wave. The COBIA likely caused bTBI due to direct PBI plus possible tertiary blast injury to the brain. With the COBIA, tertiary injury was suggested by the observation that the head was displaced by the blast, and by evidence of possible contrecoup injury involving the ventral tips of the temporal lobes, which are located directly opposite the dorsal impact site of the blast wind. On the other hand, the observation that subarachnoid hemorrhages were always present and were located predominantly in the path of the blast wave, especially after sublethal dcBI (Fig. 7A), combined with the observation that intraparenchymal hemorrhages were extremely rare, suggests that subarachnoid hemorrhages may have been due to direct PBI.

The physical mechanism by which a blast wave injures tissues is not well understood, but one mechanism believed to be involved is the deposition of kinetic energy at density boundaries. The air-water interface in the lung, the organ most sensitive to blast waves, is an important density boundary. The water-lipid interface where cerebrospinal fluid (CSF) touches the pial surface also forms a density boundary, albeit one with a lesser gradient than an air-water interface. Deposition of kinetic energy at the CSF-pial interface could rupture delicate pial venules, giving rise to widespread subarachnoid hemorrhages. Favoring this interpretation is the observation that parenchymal hemorrhages were almost invariably absent, arguing against a more generalized mechanism for hemorrhage such as transient arterial or venous hypertension. Also favoring this interpretation is that cortical contusions beneath the site of blast impact were never observed, arguing against coup injury from acceleration or from inward flexure of the skull by the blast wind as the cause of subarachnoid hemorrhage. By contrast, impact/acceleration models such as the closed head injury model of Marmarou invariably result in cortical contusion beneath the site of impact, due to coup injury or to inward flexure of the skull (Foda and Marmarou, 1994; Marmarou et al., 1994). Our direct measurements of the strain induced in the skull by the blast indicated that if inward flexure occurred, it was < 200 μm at the lambda, consistent with the observation that skull injuries were invariably absent at necropsy. At present, the best explanation for the widespread subarachnoid hemorrhages observed in our model is that kinetic energy from the blast wave was deposited at the density boundary between brain and CSF, but additional study of this hypothesis is warranted.

Blast waves generated by the COBIA

We generated blast waves by detonating smokeless powder inside of crimped brass .22 caliber cartridges. The .22 caliber cartridges were detonated inside of a commercial .22 caliber powder-actuated tool, with the tool modified by removing its piston. This modification made the tool resemble a firearm, and allowed undamped propagation of the blast wave within the barrel of the tool and into the BDC. The blast

waves generated by the COBIA bore features that are relevant to real-world explosions. At low temporal resolution, the blast waveforms from COBIA resembled simple Friedlander waves. However, at higher temporal resolution, reflections from the barrel of the tool and from the BDC resulted in complex waveforms with post-peak overpressures that resembled those recorded inside combat vehicles penetrated by munitions (Fig. 4B). The peak overpressures generated by the COBIA ranged from 250 to >1000 kPa (Table 1), with specific values determined using BDCs of different sizes and cartridges of different power levels. The peak overpressures generated by the COBIA may be compared with those generated in shock tube experiments, which typically utilize peak overpressures of 40–350 kPa for whole-body exposures (Bauman et al., 1997; Cernak et al., 2001; Chavko et al., 2007; Long et al., 2009; Petras et al., 1997; Saljo et al., 2000). Calculations based on liquid dynamic theory indicated that the velocities of the blast waves generated by the COBIA were on the order of 750 m/sec, comparing favorably to velocities calculated in simulations of humans experiencing sub-lethal air-blasts, wherein the blast wave is propagating at a velocity of 450 m/sec at the time it reaches the body (Moss et al., 2009).

The COBIA and pulmonary effects

In our experiments with sub-lethal dcBI, we observed only a small reversible effect on oxygen saturation, with all other indicators of pulmonary and other vital physiological functions remaining unaffected. In addition, histopathological examination of the lungs was unremarkable. Together, these findings indicate that the COBIA had minimal if any pulmonary effects. By contrast, whole-body as well as thorax-alone exposure of rats to lesser blast insults leads to unmistakable abnormalities involving the lungs. With whole-body exposure, one study (129 kPa) found diffuse, moderate-to-marked hemorrhage, congestion, and edema in the lungs (Bauman et al., 1997); another study (339 kPa) reported petechiae, ecchymoses, blebs, and isolated or confluent hemorrhages in the trachea and lungs (Cernak et al., 2001). With thorax-alone exposure, one study (69 kPa) found widespread areas of hemorrhage that could be confluent and involve up to 30% of the lungs; another study (304 kPa) reported a fall in mean arterial pressure, a decrease of systolic and diastolic pressures, bradycardia, and tachypnea, and a significant decrease of pH in both arterial and venous blood (Cernak et al., 1996). Given the well-documented sensitivity of the lungs to PBI, our data clearly establish that in our model, spillover of the primary insult to the lungs was minimal, and if it occurred, did not have any important physiological consequence.

The COBIA and CNS effects

Lethal blast. We found that exposures of the cranium to peak overpressures below 450 kPa were never fatal, whereas exposures to 650 kPa and higher were associated with high mortality; the LD_{50} was $\sim$ 515 kPa. Animals with lethal dcBI died rapidly of cardiopulmonary arrest following prolonged apnea. By comparison, whole-body exposure of rats to blast is associated with an LD_{50} that is 2 times smaller, 250 kPa (Richmond et al., 1961, 1962). The reason for the apparent twofold difference in sensitivity associated with cranium-only exposure compared to whole-body exposure is not known, but numerous factors could potentially contribute. First, it must be borne in mind that pressure measurements may not be standardized between laboratories. Although the Richmond data cited above indicated an LD_{50} of 250 kPa, data from another laboratory indicate that whole-body exposure to 240 kPa peak overpressure is non-lethal, causes no visible damage to the brain, and shows no evidence of damage on routine histological evaluation (Saljo et al., 2000). Additional reasons include the possibility that: (1) a certain degree of protection is afforded by the scalp and skull; (2) amplification of the blast wave occurs after it enters the torso as it propagates to the head; (3) there is added injury due to systemic effects of blast that are absent with cranium-only exposure; and (4) the cause of death with whole-body exposure does not involve the CNS exclusively. Determining the causes for the apparent differences in sensitivity will require additional investigations, including repeating experiments such as ours on rats after craniectomy.

Death following dcBI almost invariably occurred very rapidly (<1 min), and appeared to be due to primary brainstem failure without overt contusive or similar tissue-damaging injury. The rats exhibited opisthotonic posturing and apnea, both of which reflect major brainstem dysfunction. We did not attempt any pharmacological intervention, but intubation, mechanical ventilation, and cardiac massage failed to prevent cardiac arrest. Apnea is also reported with shock-tube experiments (Long et al., 2009). When examined at necropsy, the lungs and other organs except the brain appeared to be normal. Gross examination of the brain showed diffuse subarachnoid hemorrhages, but no internal brain injury. Almost invariably, animals that survived the first several minutes after blast injury did not die later; only 2 of 35 deaths were delayed.

Our findings regarding rapidity of death and pathology from fatal blast injury may be compared to reports on rats after whole-body exposure to blast. With whole-body exposure, animals that die are found to have multifocal hemorrhages in the meninges, cerebrum, and cerebellum, although whether these hemorrhages were intraparenchymal or not was unclear (Bauman et al., 1997). Also, 50% of deaths occur within 2 min, and all occur within 30 min of the insult (Richmond et al., 1962). It is not clear from available reports what the specific cause of death is following whole-body exposure to blast, but the rapid times to death (2 min) argue against entities such as malignant cerebral edema and neurogenic pulmonary edema, and favor instead primary brainstem failure involving cardiac and respiratory centers.

In humans, severe blast injury often results in delayed death that is commonly attributed to cerebral edema and brain swelling (Bauman et al., 2009; Ling et al., 2009). To our knowledge, delayed death has not been reported following blast exposure of rats, suggesting that cerebral edema and brain swelling may not be prominent effects of blast, at least not in this species. Transient edema and a modest rise in intracranial pressure have been reported in rats exposed to repeated whole-body blast, but the effects observed were small and non-lethal (Saljo et al., 2009). It appears that the threshold for blast-induced fatal brainstem injury is lower than that for microvascular dysfunction, at least in the rat. If this is also true in humans, it would suggest that cases of brain edema and swelling may actually reflect quaternary blast injury to the brain (i.e., may be due to PBI to the brain complicated by some other insult such as hemorrhage or hypotension) (DeWitt and

Prough, 2009). Understanding this complex relationship is of paramount importance because of the critical therapeutic implications.

Sub-lethal effects on neuropathology. Rats with exposure of the head alone to peak overpressures of 500 kPa or less were likely to survive. Animals that survived blast awoke from anesthesia without undue delay and typically could right themselves and sit; spontaneous activity was blunted, but they never lapsed into coma or unresponsiveness.

When examined 24 h after injury, all animals that survived the blast exhibited subarachnoid hemorrhages over the cerebrum, cerebellum, and brainstem. Subarachnoid hemorrhages were especially prominent in the path of the blast wave, and as discussed above, may have been due to physical disruption of surface venules by the blast wave itself. Subarachnoid hemorrhage is a frequent observation in humans with bTBI and is associated with worse clinical outcomes (Armonda et al., 2006), making this aspect of our model particularly relevant to the human condition. Insofar as the subarachnoid hemorrhages are diffuse, one expects that the resultant inflammatory response to the blood and blood products in the cortex would result in widespread abnormalities predisposing to delayed cognitive dysfunction.

Subarachnoid hemorrhages were observed in rats that survived exposures of 414–655 kPa. The literature suggests a rather steep pressure-response relationship for neuropathological injury in rats with whole-body exposure. Though 147 kPa overpresssure results in subarachnoid hemorrhage, necrosis, cortical cell loss, gliosis, and infiltration, exposure to 22% smaller overpressures (114 kPa) results in no detectable neuropathological changes (Long et al., 2009).

Sub-lethal dcBI was associated with abnormal immunolabeling of perfused brains for IgG, consistent with microvascular injury. The abnormalities included scattered regions of microvascular stasis and patches suggestive of vasogenic edema. However, widespread or generalized extravasation of IgG was not observed, consistent with the absence of malignant cerebral edema, the absence of brain swelling, and the near absence of delayed death. A modest transient increase in intracranial pressure to 16 mm Hg was reported after 3 successive blasts (60 kPa) over 20 min that was attributed to edema formation (Saljo et al., 2009), but overall, brain swelling and malignant edema are not prominent features in any of the rat models reported.

One important abnormality found with sub-lethal dcBI involved immunolabeling for β-APP. Both axonal and neuronal abnormalities were identified that were broadly similar to findings reported in other forms of TBI (Blumbergs et al., 1995; Bramlett et al., 1997; Itoh et al., 2009; Kilbourne et al., 2009; Pierce et al., 1996; Stone et al., 2000). Abnormalities in β-APP were widespread, and involved deep brain regions away from subarachnoid hemorrhages. The abnormalities in axonal β-APP that we observed, although quantitatively not a prominent feature of our model, likely reflect an injury similar to that identified in other studies of bTBI using silver stains (Long et al., 2009; Svetlov et al., 2010). Pronounced changes in the neuronal cytoskeleton have been reported after blast exposure, with a redistribution of neurofilament proteins in neuronal perikarya that is believed to predispose to delayed nerve cell loss (Saljo et al., 2000). In addition, the perikaryal abnormalities in β-APP that we observed correlated with Fluoro-Jade staining and abnormal nuclear cleaved caspase-3, two other markers of cell injury. Neurons in the rat brain may be injured by exposure to overpressures as low as 20 kPa (Moochhala et al., 2004), with exposure to higher levels (100–300 kPa) causing significant injury to both neuronal and glial cells (Cernak et al., 2001; Kaur et al., 1995; Saljo et al., 2010). ◀ AU1

In general, the pathological, cellular, and axonal abnormalities reported here following dcBI may account for the persistent vestibulomotor abnormalities that we observed in the accelerated Rotarod test. Previous studies with whole-body exposure to blast with body protection in rodents found that vestibulomotor abnormalities normalized within 1 week of injury (Long et al., 2009), although in other studies, abnormalities in wheel running (Bauman et al., 1997), and in an active avoidance task (Cernak et al., 2001) persisted for 5 days. Models in which functional deficits endure are particularly important because bTBI in humans is well known to be associated with long-lasting neurofunctional abnormalities (Finkel, 2006; Ling et al., 2009).

Some shortcomings of the present study should be noted. Because our primary purpose was to describe the COBIA and to use it to establish a novel model of dcBI, our characterization of the many brain abnormalities induced by the COBIA was necessarily limited. A more complete description of the neuropathological findings reported here is needed. Additional studies will be required for more comprehensive characterization of the functional, cognitive, and behavioral abnormalities induced in this model. Also, the hypothesis that subarachnoid hemorrhage is due to deposition of kinetic energy at the brain-CSF boundary calls for additional study.

In summary, we developed and validated a novel model of bTBI that is unique in allowing study of the direct effects of explosive blast on the brain, uncomplicated by indirect effects mediated via the thoracic mechanism. There is no doubt that in combat and other real-life situations, both direct and indirect mechanisms of PBI to the brain, as well as secondary, tertiary, and quarternary mechanisms, all play crucial roles in determining the overall outcome from bTBI. However, we postulate that understanding the specific contribution of each of these separate mechanisms will lead to important insights that will improve the eventual protection and treatment of the unfortunate warfighters and civilians who are victims of bTBI.

Acknowledgments

This work was supported by a grant to J.M.S. from the Department of the Army (PT074766; the U.S. Army Medical Research Acquisition Activity, 820 Chandler Street, Fort Detrick, MD 21702-5014 is the awarding and administering acquisition office). The information in this article does not necessarily reflect the position or the policy of the United States Government, and no official endorsement should be inferred.

Author Disclosure Statement

No competing financial interests exist. ◀ AU2

References

Aboutanos, M.B., and Baker, S.P. (1997). Wartime civilian injuries: epidemiology and intervention strategies. J. Trauma 43, 719–726.

Armonda, R.A., Bell, R.S., Vo, A.H., Ling, G., DeGraba, T.J., Crandall, B., Ecklund, J., and Campbell, W.W. (2006). Wartime traumatic cerebral vasospasm: recent review of combat casualties. Neurosurgery 59, 1215–1225.

Bauman, R.A., Elsayed, N., Petras, J.M., and Widholm, J. (1997). Exposure to sublethal blast overpressure reduces the food intake and exercise performance of rats. Toxicology 121, 65–79.

Bauman, R.A., Ling, G., Tong, L., Januszkiewicz, A., Agoston, D., Delanerolle, N., Kim, Y., Ritzel, D., Bell, R., Ecklund, J., Armonda, R., Bandak, F., and Parks, S. (2009). An introductory characterization of a combat-casualty-care relevant swine model of closed head injury resulting from exposure to explosive blast. J. Neurotrauma 26, 841–860.

Belanger, H.G., Kretzmer, T., Yoash-Gantz, R., Pickett, T., and Tupler, L.A. (2009). Cognitive sequelae of blast-related versus other mechanisms of brain trauma. J. Int. Neuropsychol. Soc. 15, 1–8.

Blumbergs, P.C., Scott, G., Manavis, J., Wainwright, H., Simpson, D.A., and McLean, A.J. (1995). Topography of axonal injury as defined by amyloid precursor protein and the sector scoring method in mild and severe closed head injury. J. Neurotrauma 12, 565–572.

Bochicchio, G.V., Lumpkins, K., O'Connor, J., Simard, J.M., Schaub, S., Conway, A., Bochicchio, K., and Scalea, T.M. (2008). Blast injury in a civilian trauma setting is associated with a delay in diagnosis of traumatic brain injury. Am. Surg. 74, 267–270.

Bramlett, H.M., Kraydieh, S., Green, E.J., and Dietrich, W.D. (1997). Temporal and regional patterns of axonal damage following traumatic brain injury: a beta-amyloid precursor protein immunocytochemical study in rats. J. Neuropathol. Exp. Neurol. 56, 1132–1141.

Cernak, I., Savic, J., Ignjatovic, D., and Jevtic, M. (1999a). Blast injury from explosive munitions. J. Trauma 47, 96–103.

Cernak, I., Savic, J., Malicevic, Z., Zunic, G., Radosevic, P., Ivanovic, I., and Davidovic, L. (1996). Involvement of the central nervous system in the general response to pulmonary blast injury. J. Trauma 40, S100–S104.

Cernak, I., Savic, J., Zunic, G., Pejnovic, N., Jovanikic, O., and Stepic, V. (1999b). Recognizing, scoring, and predicting blast injuries. World J. Surg. 23, 44–53.

Cernak, I., Wang, Z., Jiang, J., Bian, X., and Savic, J. (2001). Ultrastructural and functional characteristics of blast injury-induced neurotrauma. J. Trauma 50, 695–706.

Chavko, M., Koller, W.A., Prusaczyk, W.K., and McCarron, R.M. (2007). Measurement of blast wave by a miniature fiber optic pressure transducer in the rat brain. J. Neurosci. Methods 159, 277–281.

Chen, Y.C., Smith, D.H., and Meaney, D.F. (2009). In-vitro approaches for studying blast-induced traumatic brain injury. J. Neurotrauma 26, 861–876.

Clemedson, J.C. (1956). Blast injury. Physiol Rev. 36, 336–354.

Coupland, R.M., and Meddings, D.R. (1999). Mortality associated with use of weapons in armed conflicts, wartime atrocities, and civilian mass shootings: literature review. BMJ 319, 407–410.

Coupland, R.M., and Samnegaard, H.O. (1999). Effect of type and transfer of conventional weapons on civilian injuries: retrospective analysis of prospective data from Red Cross hospitals. BMJ 319, 410–412.

Courtney, A.C., and Courtney, M.W. (2009). A thoracic mechanism of mild traumatic brain injury due to blast pressure waves. Med. Hypotheses 72, 76–83.

Denny-Brown, D. (1945). Cerebral concussion. Physiol. Rev. 25, 296–325.

DeWitt, D.S., and Prough, D.S. (2009). Blast-induced brain injury and posttraumatic hypotension and hypoxemia. J. Neurotrauma 26, 877–887.

Elder, G.A., and Cristian, A. (2009). Blast-related mild traumatic brain injury: mechanisms of injury and impact on clinical care. Mt. Sinai J. Med. 76, 111–118.

Finkel, M.F. (2006). The neurological consequences of explosives. J. Neurol. Sci. 249, 63–67.

Foda, M.A., and Marmarou, A. (1994). A new model of diffuse brain injury in rats. Part II: Morphological characterization. J. Neurosurg. 80, 301–313.

Frykberg, E.R., and Tepas, J.J., III (1988). Terrorist bombings. Lessons learned from Belfast to Beirut. Ann. Surg. 208, 569–576.

Hamm, R.J. (2001). Neurobehavioral assessment of outcome following traumatic brain injury in rats: an evaluation of selected measures. J. Neurotrauma 18, 1207–1216.

Harvey, J., Nandakumar, J., and Krishnan, L.V. (1984). Dynamic calibration of shock overpressure transducers. Pramana 22, 447–451.

Itoh, T., Satou, T., Nishida, S., Tsubaki, M., Hashimoto, S., and Ito, H. (2009). Expression of amyloid precursor protein after rat traumatic brain injury. Neurol. Res. 31, 103–109.

Kaur, C., Singh, J., Lim, M.K., Ng, B.L., Yap, E.P., and Ling, E.A. (1995). The response of neurons and microglia to blast injury in the rat brain. Neuropathol. Appl. Neurobiol. 21, 369–377.

Kilbourne, M., Kuehn, R., Tosun, C., Caridi, J., Keledjian, K., Bochicchio, G., Scalea, T., Gerzanich, V., and Simard, J.M. (2009). Novel model of frontal impact closed head injury in the rat. J. Neurotrauma 26, 2233–2243.

Ling, G., Bandak, F., Armonda, R., Grant, G., and Ecklund, J. (2009). Explosive blast neurotrauma. J. Neurotrauma 26, 815–825.

Long, J.B., Bentley, T.L., Wessner, K.A., Cerone, C., Sweeney, S., and Bauman, R.A. (2009). Blast overpressure in rats: recreating a battlefield injury in the laboratory. J. Neurotrauma 26, 827–840.

Marmarou, A., Foda, M.A., van den Brink, W., Campbell, J., Kita, H., and Demetriadou, K. (1994). A new model of diffuse brain injury in rats. Part I: Pathophysiology and biomechanics. J. Neurosurg. 80, 291–300.

Moore, D.F., Jerusalem, A., Nyein, M., Noels, L., Jaffee, M.S., and Radovitzky, R.A. (2009). Computational biology—modeling of primary blast effects on the central nervous system. Neuroimage 47(Suppl. 2), T10–T20.

Moss, W.C., King, M.J., and Blackman, E.G. (2009). Skull flexure from blast waves: a mechanism for brain injury with implications for helmet design. Phys. Rev. Lett. 103, 108702.

Petras, J.M., Bauman, R.A., and Elsayed, N.M. (1997). Visual system degeneration induced by blast overpressure. Toxicology 121, 41–49.

Pierce, J.E., Trojanowski, J.Q., Graham, D.I., Smith, D.H., and McIntosh, T.K. (1996). Immunohistochemical characterization of alterations in the distribution of amyloid precursor proteins and beta-amyloid peptide after experimental brain injury in the rat. J. Neurosci. 16, 1083–1090.

Richmond, R., Clare, V.R., Goldizen, V.C., Pratt, D.E., Sanchez, R.T., and White, C.S. (1961). Biological effects of overpressures of 400 milliseconds duration and its employment in biomedical experiments. Aerosp. Med. 32, 997–1008.

Richmond, R., Goldizen, V.C., Clare, V.R., Pratt, D.E., Sherping, F., Sanchez, R.T., Fischer, C.C., and White, C.S. (1962). The

biologic response to overpressure. III. Mortality in small animals exposed in a shock tube to sharp rising overpressures of 3 to 4 msec duration. Aerosp. Med. 33, 1–27.

Saljo, A., Bao, F., Haglid, K.G., and Hansson, H.A. (2000). Blast exposure causes redistribution of phosphorylated neurofilament subunits in neurons of the adult rat brain. J. Neurotrauma 17, 719–726.

Saljo, A., Bolouri, H., Mayorga, M., Svensson, B., and Hamberger, A. (2010). Low-level blast raises intracranial pressure and impairs cognitive function in rats: prophylaxis with processed cereal feed. J. Neurotrauma 27, 383–389.

Saljo, A., Svensson, B., Mayorga, M., Hamberger, A., and Bolouri, H. (2009). Low-level blasts raise intracranial pressure and impair cognitive function in rats. J. Neurotrauma 26, 1345–1352.

Schmued, L.C., Stowers, C.C., Scallet, A.C., and Xu, L. (2005). Fluoro-Jade C results in ultra high resolution and contrast labeling of degenerating neurons. Brain Res. 1035, 24–31.

Simard, J.M., Geng, Z., Woo, S.K., Ivanova, S., Tosun, C., Melnichenko, L., and Gerzanich, V. (2009a). Glibenclamide reduces inflammation, vasogenic edema, and caspase-3 activation after subarachnoid hemorrhage. J. Cereb. Blood Flow Metab. 29, 317–330.

Simard, J.M., Yurovsky, V., Tsymbalyuk, N., Melnichenko, L., Ivanova, S., and Gerzanich, V. (2009b). Protective effect of delayed treatment with low-dose glibenclamide in three models of ischemic stroke. Stroke 40, 604–609.

Stone, J.R., Singleton, R.H., and Povlishock, J.T. (2000). Antibodies to the C-terminus of the beta-amyloid precursor protein (APP): a site specific marker for the detection of traumatic axonal injury. Brain Res. 871, 288–302.

Svetlov, S.I., Prima, V., Kirk, D.R., Gutierrez, H., Curley, K.C., Hayes, R.L., and Wang, K.K. (2010). Morphologic and biochemical characterization of brain injury in a model of controlled blast overpressure exposure. J. Trauma 69, 795–804.

Zel'dovich,Y.B., and Raizer,Y.P. (1966). *Physics of Shock Waves and High-Temperature Hydrodynamic Phenomena*. Academic Press: New York.

Address correspondence to:
J. Marc Simard, M.D.
Department of Neurosurgery
22 S. Greene St., Suite S12D
Baltimore, MD 21201-1595

E-mail: msimard@smail.umaryland.edu

APPENDIX 2
LIST OF SOPs for GLP WORK

GLP-01 Regulatory Inspection
GLP-02 Management Responsibilities
GLP-03 Study Personnel Assignment
GLP-04 Training File Maintenance
GLP-05 SOP Prep and Main
GLP-06 Training File Contents
GLP-07 Training Program Description
GLP-08 Data Entry and Corrections
GLP-09 Study File Maintenance and Organization
GLP-10 GLP Report Preparation
GLP-11 Storage and Transfer of Raw Data
GLP-12 Archiving GLP Protocols
GLP-13 Documentation of SOP, Protocol and GLP Deviations
GLP-14 Issuing GLP Protocol Amendments
GLP-15 Report Preparation for Terminated GLP Studies
GLP-16 GLP Study Related Correspondence
GLP-17 Format and Preparation of GLP Protocols
GLP-18 Equipment Maintenance and Calibration
GLP-19 Equipment Identification
GLP-20 Digital Temperature Logger
GLP-21 Test and Control Articles Receipt, Handling and Record Keeping
GLP-22 Specimen Labeling, Handling and Shipping
GLP-23 Labeling Reagents and Solutions in the Laboratory
GLP-24 Mechanisms for IACUC Protocol Review
GLP-25 Blood Collection in Rats
GLP-26 Indwelling Intravenous Catheters in Rats
GLP-27 Euthanasia
GLP-28 Necropsy Procedures
GLP-29 Weighing Rodents
GLP-30 Random Assignment of Animals to Studies
GLP-32 Equipment PZM III Precision Zoom Stereo Microscope
GLP-33 Equipment i STAT Portable Clinical Analyzer 2
GLP-34 Animal Identification
GLP-35 Assignment of Experimental Animals
GLP-37 Post Operative Animal Observations
GLP-38 Labeling
GLP-39 Responsibilities of the QAU
GLP-40 Quality Assurance Unit Training Program
GLP-41 Maintenance of QAU Records
GLP-42 Critical Phase Inspections and Data Audits
GLP-43 QAU Protocol Review
GLP-44 GLP Periodic Status Reports to Mangement and SD
GLP-45 Auditing GLP Reports

GLP-46 Maintenance of the Master Schedule
GLP-47 Internal GLP Facility Inspections
GLP-48 Equipment Laboratory Balances
GLP-49 Borrowed Rented Equipment
GLP-50 Digital Onset HOBO Data Logger
GLP-51 Equipment CyQ System Blood Pressure
GLP-52 Equipment MicroVent